nature metabolism

Review article

https://doi.org/10.1038/s42255-025-01360-4

A consensus guide to preclinical indirect calorimetry experiments

Received: 30 December 2024

Accepted: 25 July 2025

Published online: 24 September 2025

Check for updates

A list of authors and their affiliations appears at the end of the paper

Understanding the complex factors influencing mammalian metabolism and body weight homeostasis is a long-standing challenge requiring knowledge of energy intake, absorption and expenditure. Using measurements of respiratory gas exchange, indirect calorimetry can provide non-invasive estimates of whole-body energy expenditure. However, inconsistent measurement units and flawed data normalization methods have slowed progress in this field. This guide aims to establish consensus standards to unify indirect calorimetry experiments and their analysis for more consistent, meaningful and reproducible results. By establishing community-driven standards, we hope to facilitate data comparison across research datasets. This advance will allow the creation of an in-depth, machine-readable data repository built on shared standards. This overdue initiative stands to markedly improve the accuracy and depth of efforts to interrogate mammalian metabolism. Data sharing according to established best practices will also accelerate the translation of basic findings into clinical applications for metabolic diseases afflicting global populations.

First reported in 1783, indirect calorimetry is a non-invasive technique for quantifying whole-body energy expenditure by measuring the rate of oxygen consumption (VO_2) and carbon dioxide production (VCO_2) during respiration. Since the 1980s, these gas exchange measurements have been refined using computer-assisted devices[1–4]. Scientists have gained important insights into mammalian physiology using indirect calorimetry to make repeated measures under various interventions, including studies of basal metabolic rate, cold-induced thermogenesis and obesity[5–7]. Furthermore, clinical indirect calorimetry informs nutritional demands in people who are critically ill and is used to optimize exercise-performance studies[8].

Modern preclinical indirect calorimetry systems enable the detailed phenotyping of laboratory animals by supplementing gas exchange recordings with additional measurements. These systems can provide minute-by-minute monitoring of food and water intake and physical activity, together with oxygen consumption and carbon dioxide production, to track behaviour and metabolic processes with high resolution. These measurements have become indispensable in elucidating genetic, environmental and pharmacological influences on metabolism and other physiological states. Common uses for indirect calorimetry include the study of ageing-related changes in metabolism[9–12], substance abuse[13–20], bone disorders[21,22], brain circuits to study feeding and dietary patterns[23–26], cancer cachexia[27–32], cardiopulmonary disorders[33–40], control of thermogenesis through activation of the sympathetic nervous system and brown adipose tissue[41–44], drug development[45–47], energy storage and release[48–50], exercise and physical activity[51–54], inflammation and states of altered immunity[55–61], muscular dystrophies[62–65], neurological disorders[66–68], nutrition, digestion and the microbiome[69–73], sleep patterns[74–77], surgical interventions[78–81], torpor[82,83] and toxicology[84,85].

Indirect calorimetry—a field in disarray

Unlike the fields of genomics[86] or metabolomics[87], the indirect calorimetry field currently has no international organization that is responsible for establishing guidelines or standards for experiments on energy expenditure or energy balance. As the number of indirect calorimetry studies has increased, so too have the arbitrary choices in units and data analysis methods, hindering researchers' ability to compare experimental results and share data. Here, we propose establishing a series of data standards for preclinical indirect calorimetry studies. These standards will enable comparisons within the same species, which should reduce barriers to data sharing and experimental comparisons.

e-mail: asbanks@bidmc.harvard.edu

https://doi.org/10.1038/s42255-025-01360-4

Table 1 | Studies, effects and units in analysis of activin receptor signalling in mice

Correctness of unit used	Metabolic rate units	Metabolic rate phenotype	Body weight	Food intake	Genetic modification[a]	GoF or LoF	Factor	Reference
Incorrect	ml kg^{-1} min^{-1}	↑VO_2	↓	=g day^{-1}	Alb-*Inhbe* OE	GoF	Ligand	152
Incorrect	ml kg^{-1} min^{-1}	↓VO_2	↑	=g day^{-1}	Fc-ACVR2B	LoF	Receptor	153
Incorrect	ml $kg(lean)^{-1}$ h^{-1}	↑VO_2	↓	=g g^{-1} h^{-1}	aP2-*Mstn* OE	GoF	Ligand	154
Incorrect	ml $kg(lean)^{-1}$ h^{-1}	↑VO_2	↓	=kJ g^{-1} day^{-1}	*Smad3*$^{-/-}$	LoF	TF	154
Incorrect	ml kg^{-1} h^{-1}	↓VO_2[b]	↑	=g g^{-1}	*Mstn*$^{-/-}$	LoF	Ligand	94
Incorrect	ml kg^{-1} h^{-1}	↑VO_2	=	↓g 12 h^{-1}	*Mstn*$^{-/-}$	LoF	Ligand	155
Incorrect	ml kg^{-1} h^{-1}	↑VO_2	↓	ND	*Gdf3*$^{-/-}$	LoF	Ligand	156
Incorrect	ml kg^{-1} h^{-1}	↑VO_2	↓	ND	*Acvr1c*$^{-/-c}$	LoF	Receptor	157
Incorrect	ml kg^{-1} h^{-1}	↑VO_2	↓	ND	*Acvr1c*^{I195T}	LoF	Receptor	158
Incorrect	ml kg^{-1} h^{-1}	=VO_2	↓	ND	*Acvr1c*^{I482V}	LoF	Receptor	158
Incorrect	ml kg^{-1} h^{-1}	↑VO_2	↓	ND	*Smad2/3*$^{fl/fl}$::*Adipoq*^{Cre}	LoF	TF	159,160
Incorrect	ml kg^{-1} 12 h^{-1}	↑VO_2	↓	=g day^{-1}	ACVR1C mAb	LoF	Receptor	161
Incorrect	l kg^{-1} h^{-1}	↑VO_2	=	= g day^{-1}	*Acvr1c*$^{fl/fl}$::*Adipoq*^{CreERT2}	LoF	Receptor	162
Incorrect	l kg^{-1} day^{-1}	↑VO_2	↓	=g day^{-1}	*Acvr1c*$^{-/-}$	LoF	Receptor	163
Incorrect	l kg^{-1} day^{-1}	↑VO_2	↓	=g day^{-1}	*Acvr1c*$^{fl/fl}$::*aP2*^{Cre}	LoF	Receptor	163
Acceptable	ml h^{-1}	↑VO_2[b]	↑	↑g day^{-1}	*Mstn*$^{-/-}$	LoF	Ligand	94
Acceptable	ml h^{-1}	↑VO_2	=	= g day^{-1}	*Mstn*$^{-/-}$	LoF	Ligand	164
Acceptable	ml h^{-1}	↓VO_2	↑	ND	*Mstn*$^{\Delta UCP1}$	LoF	Ligand	165
Acceptable	ml h^{-1}	=VO_2	↑	↑kcal day^{-1}	Fc-ACVR2B	LoF	Receptor	166
Acceptable	ml 2 h^{-1}	↑VO_2	↓	=g day^{-1}	Alb-*Inhbe* OE	GoF	Ligand	152

[a]Activin receptor signalling regulation of metabolic rate and body weight. Signalling components affecting body weight include the ligands myostatin (MSTN), growth differentiation factor 3 (GDF3) and activin E (ActE/*Inhbe*); type 1 receptors ALK5 (*Tgfbr1*) and ALK7 (*Acvr1c*); type 2 receptors ACVR2A and ACVR2B; and transcription factors SMAD2 and SMAD3. Metabolic rate reporting should not be divided by body weight. The units reported for VO_2 are compared against the methods described in this article and in ref. 129. [b]See text for further details. [c]TSOD versus T.B-Nidd5/3 is a model of *Acvr1c* deficiency. Kg, total body mass in kilograms; kg^{lean}, lean body mass in kilograms; OE, overexpression; GoF, gain of function; LoF, loss of function; TF, transcription factor; ND, not determined or not reported. Body weight gain (↑), loss (↓) or no change (=).

Our proposed standards are designed for mouse studies; however, these guidelines are also applicable to rats, hamsters and other rodent species, if they are tested using comparable multiplexed indirect calorimetry equipment[88]. Because all mammals use O_2 and CO_2 for respiration, many of these guidelines are also appropriate for the study of larger mammalian species. Of note, however, comparisons between species using allometric scaling (a principle that describes how the characteristics of organisms change with size) do not account for differences in body composition. Moreover, within a species, body composition typically changes with body weight and requires a different set of standards[89,90]. Importantly, the body surface area-to-volume ratio affects energy metabolism, thereby resulting in a non-linear relationship between basal metabolism and body mass[91]. The smaller the animal, the larger the surface area-to-volume ratio, meaning more relative surface area to lose heat than in larger animals. This phenomenon generates a larger metabolic and thermogenic demand on smaller animals, such as mice. This difference is amplified when small mammals are studied at temperatures below thermoneutrality.

The goal of this guide is to outline best practices for analysing, visualizing and interpreting indirect calorimetry experiments involving laboratory mice, when body weights differ among comparison groups. Data standards and data-sharing frameworks have been successfully established for more recently developed technologies than indirect calorimetry. For example, the National Center for Biotechnology Information (NCBI) Sequence Read Archive (SRA) was created for RNA-sequencing data, enabling users to search for a gene of interest and query the experimental conditions that resulted in altered expression. The design of the NCBI SRA allows for easy data deposition, browsing, sharing and reuse. Integrating experimental findings that contain live, real-time mouse behaviour into a repository demands a rigorous set of standards beyond what might be required by a sequencing database, owing to the varied nature of these experiments. The fractured landscape of metabolic studies using indirect calorimetry has not yet advanced to this stage. Consequently, the pace of scientific advancement has slowed owing to unnecessary repetition and difficulty interpreting experiments. These limitations contribute to confusion and poor rigour in experimental design. Community-driven solutions are needed to collect existing preclinical findings through open-access repositories that adopt best practices in data management. Such an initiative could serve as a template for future sharing of clinical metabolic data and build on lessons learnt from successful large-scale human datasets, including the International Atomic Energy Agency Doubly Labeled Water Database[92,93].

Here, we propose that standards should be established for indirect calorimetry experiments, enabling worldwide data comparison and pooling. Larger, harmonized datasets will enable the detection of phenotypes shared between multiple genes in a signalling pathway, with patterns emerging that are not evident from individual studies. Ensuring data availability and reuse in line with community standards has the potential to accelerate basic discovery and clinical applications across biomedical research.

Establishing standardized data units

Lack of standards and consistency in data reporting

Despite the extensive use of indirect calorimetry, the field lacks standardized practices for data reporting and visualization. For example, within a single representative biological pathway (a subset of the transforming growth factor-β (TGFβ) superfamily), 8 units have been used to report oxygen consumption rates in 16 studies (Table 1). Modulation of ligands, receptors or transcription factors in this pathway can alter

https://doi.org/10.1038/s42255-025-01360-4

Table 2 | Standardized units

Metabolic parameter	Standard units[a]	Non-standard units
VO_2 or VCO_2	ml h^{-1}	ml kg^{-1} h^{-1}[b] ml $kg^{(-0.75)}$ h^{-1} ml^{-1} $kg^{(2/3)-1}$ h^{-1} ml kg(lean)$^{-1}$ h^{-1} ml^{-1} min^{-1} ml day^{-1}
Energy expenditure	kcal h^{-1}	Watts (J s^{-1})[c] kcal h^{-1} kg^{-1} kJ/h
Energy intake[d]	kcal h^{-1}	kcal day^{-1} kcal kg^{-1} h^{-1}
Water intake	ml h^{-1}	g h^{-1}
RER	No units	No units
Physical activity	Metres[e]	Beam breaks

[a]The choice of standardized units is contentious. Many of the early mouse experiments reported units in ml kg(body weight)$^{-1}$ h^{-1}—a practice now abandoned owing to the artefacts introduced when dividing by body weight. Any correction for body weight is done in the statistical analysis (with ANCOVA) and not by dividing by body weight. Despite a well-reasoned proposal to report results in the International System of Units (SI) units of kJ and Watts, this practice has not been widely adopted[88]. We therefore propose kcal h^{-1} as the de facto standard. [b]The kg term refers to the body weight of the animal in kilograms, or the lean body mass in kg as indicated. [c]The SI unit of energy is the Joule (J) and J per second is Watts (W). [d]Calculated using the metabolizable calorie content (for example, food in grams h^{-1} × diet in kcal $gram^{-1}$). [e]Not all systems report distance in metres.

metabolic rates, thereby contributing to variations in body weight. The inconsistent use of units across studies complicates direct comparisons between experiments.

In our representative example pathway, selected studies include effects on ligands: myostatin (*Mstn*), activin E (*Inhbe*) and growth differentiation factor 3 (*Gdf3*); the type 1 activin receptor ALK7 (*Acvr1c*), a type 2 activin receptor ligand trap Fc-ACVR2B; and tissue-specific knockouts of the transcriptional mediators of this pathway, SMAD2 and SMAD3 (Table 1). In this selection, we find a variety of units reported for oxygen consumption (VO_2), including: ml kg(lean mass)$^{-1}$ h^{-1}; ml kg^{-1} h^{-1}; l kg^{-1} h^{-1}; l kg^{-1} day^{-1}; ml kg^{-1} min^{-1}; ml kg^{-1} 12 h^{-1}; ml 2 h^{-1}; and ml h^{-1}. Of these, only the latter two units are free from the artefacts introduced by dividing metabolic rates by body weight. Maintaining multiple separate unit systems for a single measurement is counterproductive. Furthermore, these examples raise the practical issue of whether the results can be compared. Unfortunately, directly comparing the effects of models reported with different units becomes impossible without access to individual animal body-weight data.

Of particular interest is a study of *Mstn*$^{-/-}$ mice[94]. *Mstn*-deficient mice have lower fat mass, greater lean mass and greater total mass than do wild-type mice. The authors presented two analyses of metabolic rate with opposite conclusions. When VO_2 is not normalized to body weight (ml h^{-1}), the highly muscular *Mstn*-deficient mice display greater VO_2 than that of control mice. However, when VO_2 is divided by body weight (ml kg^{-1} h^{-1}), the VO_2 value is now decreased in *Mstn*-deficient mice, and this finding is the result described in the abstract[94]. Examples similar to this one are pervasive, as seen with loss-of-function models of growth hormone (*Gh*), growth hormone receptor (*Ghr*)[95–97], leptin (*Lep*$^{ob/ob}$)[4,98], melanocortin 4 receptor (*Mc4r*)[99] and interleukin 10 (*Il10*)[100,101]. These discrepancies highlight the need for uniform standards to report and analyse data from indirect calorimetry experiments. We propose a set of standardized units, in which the practice of dividing metabolic rates by body weight is discontinued (Table 2).

Data formats and processing

Preparing data for analysis is often more challenging than the analysis itself, owing to the different data formats and the non-linear nature of physiological recordings. Currently, three main commercial entities manufacture preclinical indirect calorimetry systems (that is, Sable Systems, TSE Systems and Columbus Instruments). Each system provides distinct data file formats and units for the same fundamental measurement. For example, these systems report VO_2 results in ml min^{-1}, ml $kg^{(-0.75)}$ h^{-1} and ml kg^{-1} h^{-1}, respectively. The many different units reflected in the literature probably stem from the different output formats of these systems. A free web-based tool, CalR, can read and analyse data in formats native to these manufacturers and produce a standardized output file. CalR enables investigators with no programming experience or in-depth statistical training to reproducibly perform visualization and statistical analyses of indirect calorimetry experiments[102]. The CalR program uses our proposed set of standardized units (Table 2). Hundreds of publications have used CalR, helping to establish standards in the literature. This program can serve as a template for standardized data visualization and analysis.

Indirect calorimetry studies can be designed to explore everything from basal, steady-state metabolism to pharmacologic interventions, dietary choices, physical activity measured on running wheels, stable-isotope studies, fasting and refeeding, changes to ambient temperature and many other possibilities. As such, the design of these experiments can vary widely. We propose analysis standards based on a straightforward example of two groups of animals measured under steady-state conditions with no additional intervention during the study. More complicated studies can utilize the same proposed standards, but also necessitate detailed, time-stamped records of interventions and variables. Moreover, new data analysis tools can be created that can help investigators to reanalyse previous experiments. It is therefore crucial that metadata describing any experimental interventions are included with the raw data (Table 3).

Standardized data visualizations

Data visualization should help the reader to understand the underlying biological system and promote clear interpretation. We present a series of visualizations from a common model of diet-induced obesity[103], which can serve as standards for experiments involving altered body-weight regulation (Fig. 1). Our analysis includes data from a group of genetically identical littermate male C57BL/6J mice maintained on either a control low-fat diet (LFD) or an obesity-inducing high-fat diet (HFD). These data are collected as part of the Mouse Metabolic Phenotyping Working Group, as described previously[104]. Comprehensive metadata for this experiment are also presented (Table 3).

Visualizing indirect calorimetry experiments: body composition

Body weights of mice on a HFD increased more rapidly than did those of mice on a LFD (Fig. 1a). In the final 4 weeks of the study period, the rate of weight change is linear at a rate of 0.4 and 1.4 g $week^{-1}$ for LFD or HFD, respectively. Determining body composition helps us to understand whether these changes are attributable to differences in fat mass or lean mass. Here, whole-body quantitative NMR (qNMR, for example, EchoMRI or Bruker) measures grams of lean and fat mass without the need for anaesthesia. However, this technique does not detect the approximately 5–25% body mass that corresponds to bone or skin[105]. A DEXA scan returns similar results for fat mass and fat-free mass inclusive of bone, but generally requires anaesthesia.

Body composition data are represented either as absolute tissue masses in grams (Fig. 1b) or as a percentage of total mass (Fig. 1c). The first plot demonstrates that the greater body weight of HFD-fed mice is due to increased amounts of fat mass, with similar quantities of lean mass. Plotting these data as a percentage of body composition can be misleading (Fig. 1c). This plot shows that HFD mice have an increased percentage of body fat, but also that HFD mice have a lower percentage of lean mass. However, this representation does not accurately reflect

https://doi.org/10.1038/s42255-025-01360-4

Table 3 | Metadata essential for data sharing

Information	Example of metadata	Comments
Animal		
Species	Mouse	To maximize the potential for data sharing and reuse, a robust set of metadata is included for each animal and experiment. Animal information should include body weights at the start and conclusion of the experiment. These data can be used as a quality-control check for malfunctioning equipment[110]. When available, information on body composition, as measured by DEXA scan or whole-body qNMR can help to analyse experiments with significant differences in body weight.
Genetic background	C57BL/6J	
Strain and genotype	Wild type	
Tissue specificity	N/A	
Age at measurement (or date of birth)	18 weeks	
Sex	Male	
Body weight at start	Yes	
Body weight at end	Yes	
Body composition at start[a]	No	
Body composition at end[a]	Yes	
Litter size	N/A	
Experimental		
Intervention or treatment	HFD for 10 weeks	Experimental information will describe the experimental design or link to a publication. Ambient temperature is essential metadata because it has a strong effect on rodent physiology[167]. A quality score, based on completeness of data and metadata for each experiment, experimental sample size and duration, is awarded. These metadata are consistent with the ARRIVE guidelines 2.0 for reporting animal research[168].
Diet manufacturer	Research Diets	
Diet catalogue number	LFD: D12450B, 10% kcal fat HFD: D12452 60% kcal fat	
Caloric value	LFD: 3.82 kcal g^{-1} HFD 5.21 kcal g^{-1}	
Cage or ambient temperature	Cage temperature 24.3 ± 0.2 °C	
Photoperiod	Light 0600/1800	
Calorimetry date (YYYY/MM/DD)	2015/02/20–2015/02/23	
Batches or combined runs	2 batches	
Number of animals	16 per group, 32 total	
Unique identifier	CalR0000182	
Ethics statement	Yes	
Investigator	Lantier, McGuinness	
If available, institution or location	Vanderbilt	
Calorimetry equipment	Sable, Promethion	
Bedding	Alpha-dri	
EE calculation method	Weir[116]	
Acclimation time	18 h	
Enrichment (such as wheels, igloo)	Body mass hopper enclosure	
Publication	Corrigan et al.[104]	

[a]Where available. N/A, not available; EE, energy expenditure; ARRIVE, Animal Research: Reporting of In Vivo Experiments.

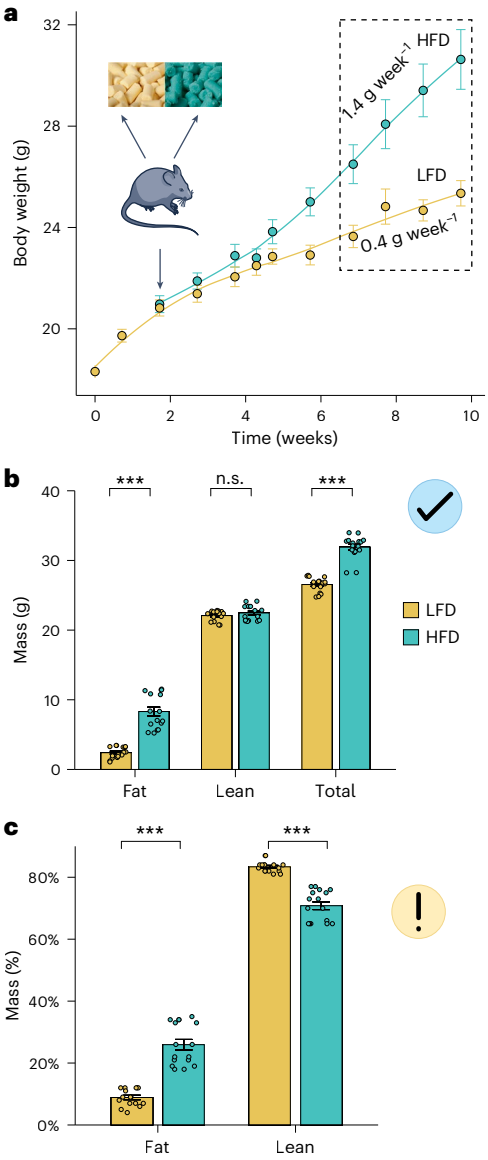

Fig. 1 | Standard visualizations of body composition in diet-induced obesity. Littermate male C57BL/6J mice were divided into two equal groups at week 2 to receive either a HFD (green) or LFD (yellow). **a**, Weekly group averages for body weight (g) of mice on the LFD or HFD. The dashed box represents stable weight change in both groups. The slopes of weight change per week are indicated. Body composition was determined at the conclusion of the study. **b**, Plot of body composition showing the absolute amount of fat, lean and total mass (g). Other body mass (for example, bone and skin) that was not detected by qNMR is not shown. **c**, A plot showing percentage body composition, which might be misinterpreted to indicate a lower absolute amount of lean mass in HFD-fed mice. The tick and warning icons in **b** and **c** indicate appropriate and inappropriate analyses, respectively. Statistical comparisons by unpaired *t*-test. ***$P < 0.001$, n.s., not significant, $n = 16$ mice per group. Data are shown as mean ± s.e.m.

the fact that HFD mice and LFD mice actually have similar amounts of lean mass. In most cases, representations of percentage body composition should be shown only when the absolute masses are also provided[97,106]. In this example, the greater weight of genetically identical mice on a HFD corresponds primarily to additional fat mass. Body composition analysis should be performed when there are weight differences between groups. This analysis is critical as laboratories move towards the use of outbred mouse models, such as diversity outbred mice. Here, the goal is to study the heterogeneous response to an intervention on a background in which there are large intrapopulation genetic contributions to phenotypic variation, similar to humans.

Visualizing indirect calorimetry experiments: energy intake, expenditure and balance

Indirect calorimetry can help investigators to understand the source of the differences in body weight or body composition between groups of animals. Body weight differences can arise from changes in energy

https://doi.org/10.1038/s42255-025-01360-4

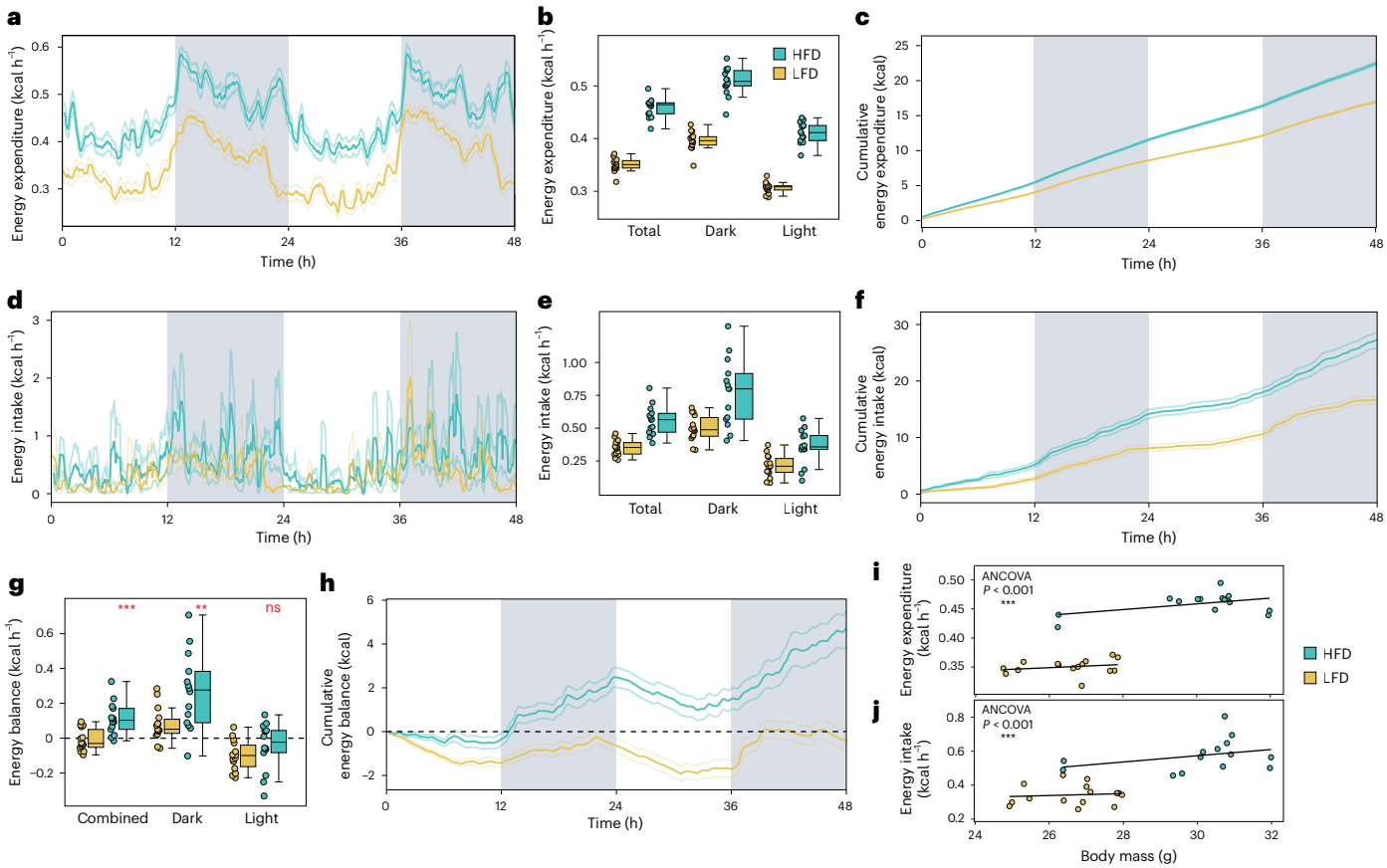

Fig. 2 | Visualizing indirect calorimetry results. In an ideal experimental scenario, indirect calorimetry would be performed before body weights had diverged. In this example, body weights of littermate male C57BL/6J mice are significantly different between groups (HFD, green; LFD, yellow). **a**–**j**, Plots of energy expenditure (kcal h^{-1}), energy intake (kcal h^{-1}), energy balance (kcal) and statistical analysis over 48 h (grey bars indicate dark photoperiods). Ten weeks after randomization to HFD or LFD, the mice were placed in an indirect calorimeter. Data versus time are plotted as the group mean ± s.e.m. for each diet, as represented by the line and ribbon, respectively. Data are plotted every 5 min with a 6-point rolling-window (30-min) smoothing function applied to the visualizations, but not to values for statistical analysis. **a**, Energy expenditure versus time. **b**, Boxplots representing the 25th percentile, median and 75th percentile of the daily energy expenditure per mouse. Points represent each mouse. **c**, Cumulative energy expenditure. **d**, Energy intake (that is, food mass × energy content of food) versus time. **e**, Boxplots representing the daily mean energy intake per mouse. **f**, Cumulative energy intake. **g**, Energy balance (metabolizable energy intake minus energy expenditure); average values for dark, light and combined photoperiods are shown. For statistical analysis, ANCOVA was used. **h**, Cumulative energy balance versus time. **i**,**j**, Statistical analysis by ANCOVA for energy expenditure and energy intake, with body mass as a covariate. In both cases, the groups are statistically different. A mass × group interaction effect was not significant. $^{**}P < 0.01$; $^{***}P < 0.001$.

intake, energy expenditure, energy absorption and energy excretion. The calculation of energy balance is the energy intake (for example, in kcal) minus energy expended minus any non-absorbed calories. Integrating changes in both energy intake and expenditure provides a more sensitive measure of energy balance and how it affects body weight than can either measurement alone. To obtain energy intake values, we multiply the amount of food consumed in grams by the metabolizable energy content of the food in kcal g^{-1}, as provided by the manufacturer. To obtain energy expended, we use indirect calorimetry, as discussed. To obtain the caloric content of any non-absorbed calories, we use bomb calorimetry to determine the energy content of the excreted faeces[107].

Here, we demonstrate a simplified example of energy balance solely using food intake and energy expenditure, in mice fed a LFD or HFD (Fig. 2). In general, mice with greater masses have a higher metabolic rate than do mice with lower masses. This observation on the effect of body size also holds in people with obesity (who tend to have more total mass), who have an increase in oxygen consumption compared with lean control individuals (who tend to have less total mass)[6,108]. In our mouse model, we represent energy intake and expenditure versus time: at each measurement instance; as a daily average; and as the cumulative value over 48 h. We find HFD-fed mice exhibit a consistently higher rate of energy expenditure than do LFD-fed mice (Fig. 2a–c). The HFD chosen for this study increases energy intake in C57BL/6 mice[109]. These differences in energy intake are not as apparent in instantaneous plots (Fig. 2d). However, the cumulative energy intake over 48 h shows the divergence in total food consumed (Fig. 2e,f). Both the average and cumulative energy balance plots show the divergence between groups occurs primarily during the dark photoperiods (Fig. 2g,h). Visualizing energy balance is helpful when groups of animals have significant differences in both energy intake and expenditure (Fig. 2i–j). These differences in energy balance are predicted to drive changes in body weight. The key points to take into account in analyses such as these are: first, to understand the energy content of the diet and plot the energy intake in kcal rather than in grams; and second, to avoid 'normalizing' by body weight. These visualizations demonstrate HFD-fed mice have both increased energy intake and energy expenditure. The slightly greater energy intake versus expenditure leads to positive energy balance and weight gain.

Quality control, limitations and technical bias

Quality control. Indirect calorimetry systems are complex machines that are prone to failure. During the study, we recommend that real-time monitoring is performed to identify and correct any malfunctions with

https://doi.org/10.1038/s42255-025-01360-4

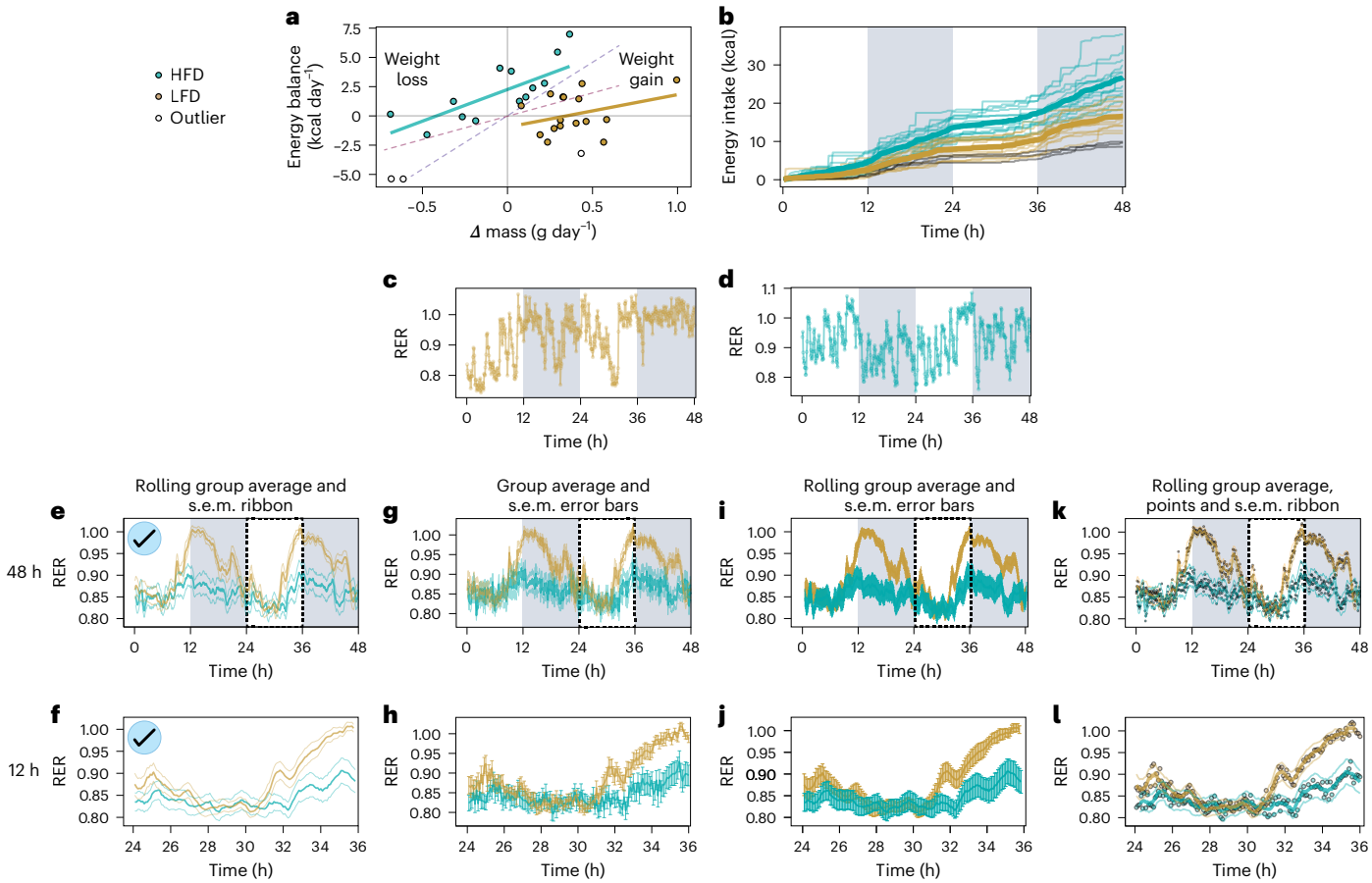

Fig. 3 | Quality control and visualization guide. a,**b**, Quality control in indirect calorimetry experiments of littermate male C57BL/J mice on a HFD (green) or LFD (yellow) (grey bars indicate dark photoperiods). **a**, The mass change (*Δ* mass) is determined from measurements taken before and after the indirect calorimetry experiment. Calculated daily energy balance (kcal day^{-1}) versus *Δ* mass for each animal over 48 h. The three cages with malfunctioning feeders are excluded from the analysis (open circles). Linear regression is predicted to cross the origin (dashed line) with slope of 4 kcal g^{-1}, corresponding to weight change from lean mass (pink), or slope of 9 kcal g^{-1}, corresponding to weight change from fat mass (purple). **b**, Cumulative food intake (kcal) for each mouse, overlayed with group means. The values for the three excluded mice are shown in black. **c**–**l**, Visualization guide. Plots of the RER, the ratio of VCO_2 to VO_2 and an indicator of substrate oxidation (1.0 corresponds to more carbohydrate oxidation, 0.7 corresponds to more fatty acid oxidation). Mice on a HFD have more fatty acid oxidation and a lower RER than do mice on a LFD. **c**,**d**, The RER for one mouse on a LFD (**c**) or one mouse on a HFD (**d**). Group mean values of RER versus time for 48 h (**e**, **g**, **i**, **k**) or 12 h (**f**, **h**, **j**, **l**) (corresponding to the dashed box). Plotting choices include the visualization of ribbons or error bars to represent the s.e.m. and raw group mean values or a 6-point rolling average (30 min smoothing). **e**,**f**, Lines represent group means ± s.e.m. with ribbons and smoothing. This is our recommended visualization (indicated with the tick icons). **g**,**h**, Lines represent group means ± s.e.m. with error bars and no smoothing. **i**,**j**, Lines represent group means ± s.e.m. with error bars and 30-min smoothing. **k**,**l**, Points and lines represent group means ± s.e.m. with ribbons and smoothing.

the equipment. At the conclusion of recording, data should be examined for common problems. An exploratory data analysis should be performed on each of the parameters measured by the indirect calorimeter[110]. An effective approach to quality control includes recording the body mass change of each animal before and after the study, using a laboratory balance, against the calculated energy balance derived from the indirect calorimetry system (Fig. 3a). Mice with a positive energy balance (energy balance > 0) should gain weight (*Δ* mass > 0). Conversely, mice with a negative energy balance (energy balance < 0) should lose weight (*Δ* mass < 0). The strength of this approach is that gross outliers that might have been missed during the experiment, or in the original examination of the raw data, can be identified for further scrutiny. We present an example in which malfunctions in three food hoppers caused food to become inaccessible during an experiment (Fig. 3b). In these three cages, we saw data consistent with a jammed feeder, which led to causing fasting-like behaviour for more than 12 h: little or no food intake and lower respiratory exchange ratio (RER), corresponding to increased fatty acid oxidation[111]. We concluded that these data differ significantly from those from the other cages, and although they are included in the dataset, they are excluded from the analysis.

Limitations. The limitations to indirect calorimetry experiments include the inability to detect altered energy absorption or excretion. Differences in energy absorption between diets or groups of mice can affect energy balance. In addition, the calorie content of diets that is accessible to digestion (the 'metabolizable energy') is an approximation provided by manufacturers and could exhibit considerable variation between batches. Experiments with multiple synthetic diets are likely to compound these errors[107,112]. Furthermore, the energy-balance calculation might need modification if other parameters are involved, such as additional intake calories from other sources (for example, sucrose-sweetened water) or additional calories lost owing to glycosuria[113,114].

In this simplified example, we find LFD-fed mice gaining weight despite a prediction for a negative energy balance. In the HFD-fed group, we find mice with a positive energy balance that have essentially no mass change. Possible explanations for the deviation from the expected theoretical values include an underestimation of the metabolizable energy in the LFD, an overestimation of metabolizable energy in the HFD or increased food spillage owing to the crumbly texture of the HFD. In cases in which the groups are expected to have

https://doi.org/10.1038/s42255-025-01360-4

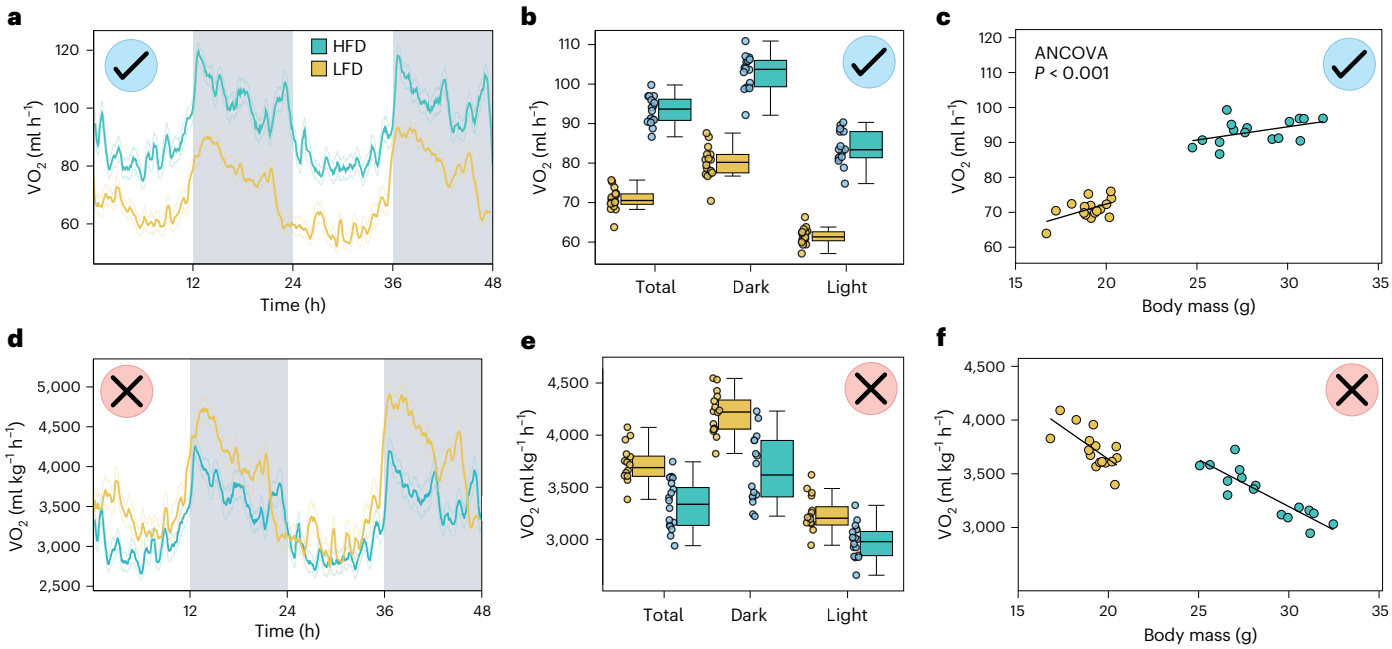

Fig. 4 | Correct and incorrect visualization of metabolic rates. In a second cohort of littermate male C57BL/6J mice on a LFD (yellow) or HFD (green), plots of the average VO_2 versus time; boxplots with the median, 25th percentile and 75th percentile over 48 h; and regression plots of the VO_2 versus total body mass. **a**–**c**, The standard visualization of metabolic rate (VO_2 in ml h^{-1}), with no normalization applied (tick icons indicate that this is our recommended visualization). **d**–**f**, An incorrect and misleading visualization achieved by dividing VO_2 by total body weight (VO_2 in ml kg^{-1} h^{-1}). With this erroneous manipulation (indicated with cross icons), mice with the largest mass now appear to have the lowest metabolic rate. Dividing by total body weight assumes that the groups of mice have homogeneous body compositions; this assumption is violated in this example, because mice on a HFD have greater fat mass than do mice on a LFD.

altered energy absorption or excretion, faecal bomb calorimetry can help to more precisely define differences in energy balance[107,115]. Preclinical energy expenditure is often estimated using the simplified Weir equation, which assumes stable body weight. A more precise but onerous estimate of energy expenditure involves measuring urinary protein excretion to quantify nitrogen balance[116]. When the mass and energy changes of the system do not add up, it is worth revisiting the experiment's assumptions and limitations.

Technical bias. A major limitation of indirect calorimetry experiments are the technical issues that can contribute to reduced replicability of experimental results[104]. Whether differing results between investigators and institutions are caused by technical errors or environmental considerations (such as ambient temperature, humidity or noise) is not clear. Assuming the system is accurately calibrated, common technical errors include mechanical issues, such as loose connections of gas tubing to cages, wires obstructing activity beams and scales falling out of range; cages being opened during measurements, causing spikes in the gas data; and unplanned disruptions to the light–dark cycle or ambient temperature. Alternative, intrinsic explanations can include differences in the microbiome, effects of different indirect calorimetry equipment, diet composition and bedding differences affecting behaviour[117]. Last, systemic noise can affect the ability to detect feeding behaviours owing to mice establishing food caches, thereby limiting the sensitivity of indirect calorimetry experiments to detect small differences between groups.

Other styles: smoothing, error bars, shading, groups and individuals

Plots of indirect calorimetry data represent attempts to clearly visualize hundreds of data points. As an example, we present the RER (that is, VCO_2/VO_2), a measure of substrate oxidation in vivo. The physiological state of individual animals exhibits large daily fluctuations. Although plots of representative animals can be informative (Fig. 3c,d), overall trends between animals on different diets can become more evident when taking group averages[15,88]. In our example, we see mice consuming a high-carbohydrate LFD have greater RER values in the dark photoperiod, corresponding to increased carbohydrate oxidation concurrent with periods of increased food intake. By contrast, HFD-fed mice have more fatty acid oxidation and a lower RER (Fig. 3e).

Plot smoothing. We recommend visualizing a time course as a rolling average to reduce the visible scatter caused by the activities of individual animals. Of note, smoothed data are for illustration purposes only, and the unsmoothed data are used exclusively in statistical analysis. In this example, the raw data are presented every 5 min. We demonstrate a 30-min (6-point) rolling average window for 48-h and 12-h plots. In addition, to simplify the visualization, we recommend plotting the s.e.m. as a ribbon (Fig. 3e,f).

Error bars versus ribbons. Plotting ribbons to show the s.e.m. is an improvement over the common time-course visualization, in which positive and negative error bars demonstrate the s.e.m. (Fig. 3g–j). A drawback to this visualization is that error bars can overlap, masking mean values. Overplotting, or overlap of plotting elements, is more notable for a 48-h visualization than for a 12-h plot. Plotting ribbons allows us to avoid plotting error bars every 5 min for 48 h, or 576 positive and negative error bars for each diet. The ribbons present a less-crowded plot, especially for high-resolution measurements. This combination of rolling group average and s.e.m. ribbons is the preferred visualization used throughout this example. The value of each average point per group can also be valuable (Fig. 3k,l).

Which plots to include?

We recommend presenting the values for energy expenditure, energy intake, RER, activity and body composition. The VO_2 and VCO_2 values are closely related and qualitatively appear nearly identical. In addition, because VO_2 and VCO_2 are used to calculate energy expenditure,

presenting all three plots is somewhat redundant, and additional plots can be shown in the supplementary materials. With the implementation of a data repository, authors might feel less urgency to present plots from each measurement in an indirect calorimetry experiment, given that the full dataset will be available to the community.

Standardized data analysis

Analysis standards: common mistakes

Attempts to normalize metabolic rates can obscure important biological trends (Table 1). To illustrate this issue, we present VO_2 data with two different treatments (HFD versus LFD) in a second cohort of mice. Non-normalized VO_2 data in units of ml h^{-1} allow for an accurate representation of the results (Fig. 4a). Using ml h^{-1}, the VO_2 versus time plot clearly indicates that HFD-fed mice have a higher metabolic rate than do LFD-fed control mice. Boxplots of the average hourly VO_2 levels over 48 h also reveal increased values in HFD-fed versus LFD-fed mice (Fig. 4b). However, these values in the boxplots are unsuitable for statistical analysis of mass-dependent variables because they do not account for body mass. A regression plot of mean VO_2 versus total body mass highlights that the metabolic rate of HFD-fed mice in relation to total body mass is greater than that of LFD-fed mice, and statistical analysis with analysis of covariance (ANCOVA, discussed in the next section) shows a significant difference between the groups (Fig. 4c).

The practice of normalizing metabolic rates (energy expenditure, VCO_2, or VO_2) by dividing by body weight is incorrect (Fig. 4d–f). There is no acceptable justification for this analysis if the average body masses and/or body composition are different between test groups, because this can produce misleading findings. The metabolic rates could be divided by total body weight only when the groups of mice being compared have similar body compositions, that is if both groups have the same percentage of lean and fat mass. Furthermore, if body composition is similar between groups, then there is no need to divide VO_2 by body weight. In our example, this practice leads to the misleading representation that HFD-fed mice have lower rates of VO_2 than LFD-fed mice (Fig. 4d,e). Moreover, a regression plot of VO_2 in units of ml kg^{-1} h^{-1} versus body mass is confusing (Fig. 4f). This plot suggests that the largest mice should have the lowest metabolic rates. The dramatic reversal of experimental interpretation illustrates how the choice of analysis method can change the conclusions.

ANCOVA over and over again

The greatest strength of indirect calorimetry in preclinical models is the de facto consensus method for statistical data interpretation, ANCOVA[108,118–130]. This technique's advantages include its ability to handle the comparison of animals with different body compositions (for example, increased fat mass in obesity or decreased muscle mass in ageing). ANCOVA has well-documented statistical foundations and is readily accessible through software tools, allowing for ease of implementation. This analysis is used to determine statistical differences between groups for body mass-dependent parameters, including VO_2, VCO_2, energy expenditure, energy intake and water intake. These mass-dependent variables are defined as having an effect proportional to body mass, that is larger mice have a greater energy expenditure than do smaller mice. This effect is important to consider when analysing mass-dependent variables. Detailed descriptions of the mathematical basis for ANCOVA are available[129,131].

When conducting an ANCOVA, it is important to test whether the slopes (for example, energy expenditure versus mass) are parallel between groups. This assessment requires a statistical test for an interaction between groups and the covariate. In many cases, the interaction effect will not be significant, the slopes will be nearly parallel and an ANCOVA can be performed. However, if there is a significant interaction effect between groups and the covariate, it implies that the association of the group with the dependent variable (for example, energy expenditure) is not constant across levels of the covariate (for example, mass)[132]; therefore, there is no single answer to the question of which group is higher and by how much (Fig. 5a). In the event that a significant interaction effect is observed, additional statistical approaches are possible, including the general linear model[102,124,132,133]. If the slopes are parallel, ANCOVA can be used for the analysis and the interpretation is straightforward (Fig. 5b). Additional details, examples, benefits and limitations of ANCOVA have been described in detail[102,108,123,124,129,131,134].

ANCOVA has been an effective analysis standard for more than a decade. Although many studies use this method, a variety of units and analysis methods reporting metabolic rates are still used (Table 1). The underlying reasons for the lack of consistency could derive from the default output units used by different phenotyping systems or from historical inertia. However, the blame for the fragmented state of the field rests on our failure as investigators to self-organize and determine acceptable and unacceptable standards. No rational argument has been made for 'normalizing' by body weight (Fig. 4d), and we propose that this practice is ended in preclinical indirect calorimetry experiments.

Statistical significance is assessed with the ANCOVA using a mass variable as the covariate. One important question is which covariate should be used. The total body mass incorporates lean mass, fat mass and other components. By default, we use the total mass as the covariate. In our example, a plot of energy expenditure versus total mass shows that the HFD and LFD groups have similar slopes and different *y* intercepts, a reflection of the complexity of the model (Fig. 5c). The argument to use lean mass as the covariate stems from lean tissue constituting much of the body mass and being more metabolically active than fat tissue[126,135]; however, the main drawback is that this ignores the contribution of fat mass to metabolic rate. In this example, some HFD-fed mice have more than 30% body fat. Similarly, using fat mass as the covariate ignores the contribution of lean mass to energy expenditure, an assumption that is rarely acceptable. Here, the plot of energy expenditure versus lean mass results in nearly parallel slopes, with an offset in the *y* intercept (Fig. 5d). One interpretation of this plot is that lean mass is driving the effect on whole-body energy expenditure. The different *y* intercepts account for non-lean mass components. When fat mass is used as the covariate, in this example, we see that most LFD-fed mice have a small amount of fat mass, less than 10% of body composition. The increasing amounts of fat mass only make a minor contribution to energy expenditure in these mice, housed at 23 °C. In this experiment, fat mass is a poor independent predictor of energy expenditure (Fig. 5e). Finally, to assess the contributions of both lean mass and fat mass to metabolic rates, we could use multiple linear regression, with energy expenditure as the dependent variable and both lean mass and fat mass as independent variables. However, lean mass and fat mass are often correlated and are not independent[126] (Fig. 5f).

Addressing the issue of collinearity of lean and fat mass in the analysis of metabolic rates is an open area of investigation. As we perform linear regression for energy expenditure versus lean mass, we find a significant contribution, but we do not find a significant contribution of fat mass to energy expenditure. This difference is not surprising, with the lower metabolic rate of fat compared with lean mass and a relatively small contribution to body composition. In this example, we use either lean mass or total mass (Figs. 5c,d) as acceptable covariates. Both produce a statistically significant effect of diet on energy expenditure. This finding suggests that the effect of ignoring fat mass when using lean mass as the covariate does not negatively influence the model in this example.

The need for a shared indirect calorimetry data repository

There are ongoing reproducibility and replicability concerns in obesity, nutrition and metabolic research[136–138]. We propose creating a data repository that enables investigators to deposit their indirect calorimetry results, thereby facilitating comparisons between different datasets. With the cooperation of funding bodies, journals

https://doi.org/10.1038/s42255-025-01360-4

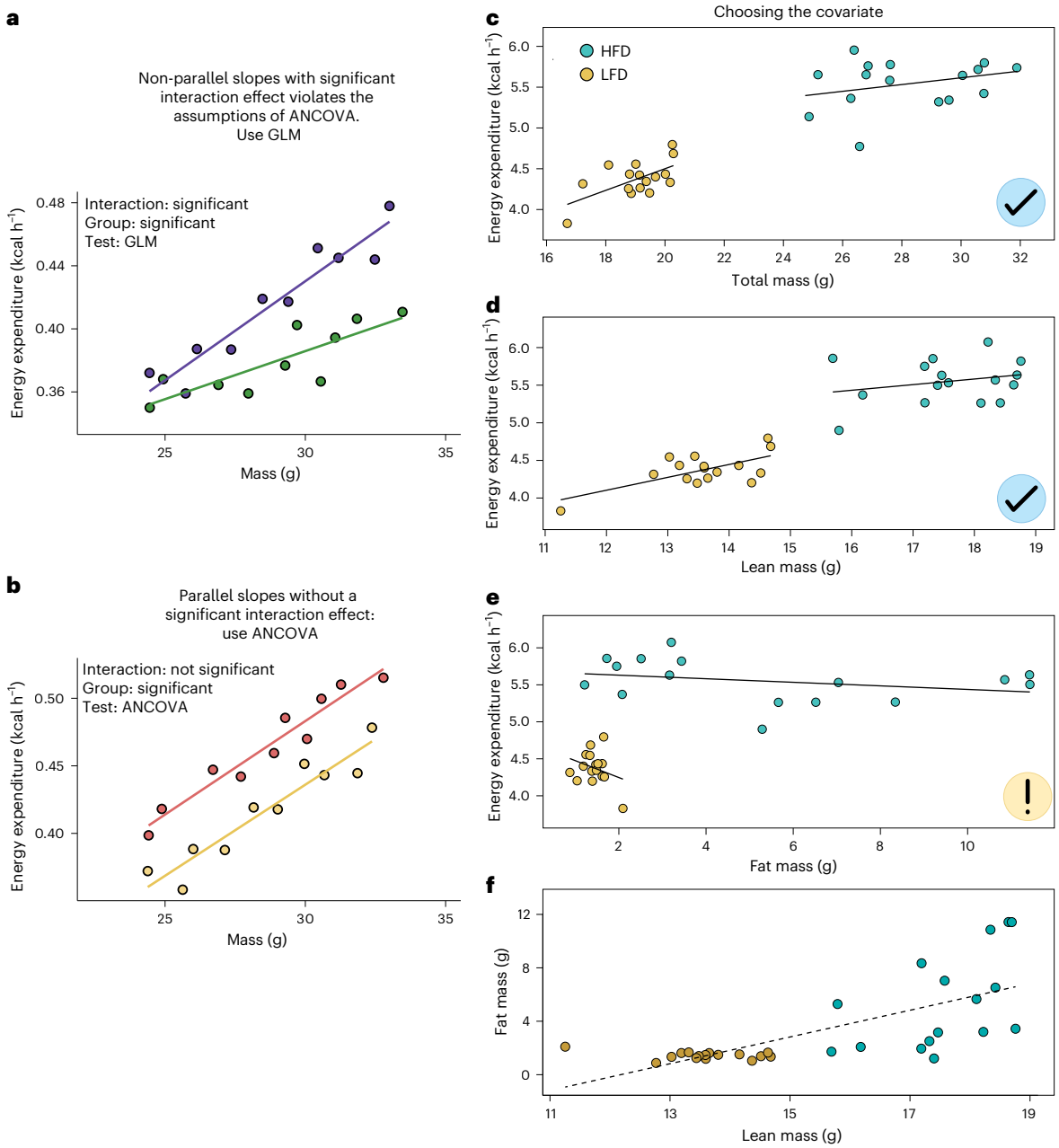

Fig. 5 | Statistical approach for indirect calorimetry and choosing the appropriate covariate. a,**b**, Statistical tests. For analysis of mass-dependent variables (for example, energy expenditure or VO_2), we first perform a statistical test to determine whether the slopes are parallel, by testing for an interaction effect between the covariate (total mass) and the group variable. In example 1 (**a**), the non-parallel lines produce a statistically significant interaction effect and dictate that ANCOVA cannot be used in this analysis. The diverging lines make the interpretation of the experiment more complex; the statistical differences between the groups will depend on the specific mass range at which the comparison is made. For statistical analysis, we will use the general linear model (GLM) when an interaction effect is significant. In example 2 (**b**), we first run a test for the interaction effect and find that it does not reach statistical significance. This result allows us to proceed with ANCOVA. **c**–**f**, Comparison of energy expenditure (kcal h^{-1}) as the dependent variable versus different mass covariates as the independent variable. **c**, Energy expenditure versus total mass (g). **d**, Energy expenditure versus lean mass. **e**, Energy expenditure versus fat mass. **f**, There is a positive correlation (dashed line) between the two independent variables, fat mass versus lean mass. This correlation complicates the use of lean and fat mass as multiple independent variables for regression.

and reviewers, we aim to standardize and unify the field, accelerating physiology research globally. The prevailing assumption that data are 'available upon reasonable request' is often unfounded[139]. This resource would also help researchers comply with data management and sharing plans mandated by funding bodies.

A data repository

The data repository will adhere to 'findability, accessibility, interoperability, and reuse of digital assets' (FAIR) data principles[140]. Every dataset uploaded by the community will comply with metadata standards (Table 3). These standards will include a persistent data identifier to permanently reference a dataset on the web for indexing by search engines and tracking data reuse. For accessibility, the data will be available to anyone locating that record. Interoperability will permit all data in the calorimetry database to work in the same framework. Most importantly, reusing experimental data will allow for datasets to be shared and unnecessary duplication of efforts to be reduced, in addition to minimizing the use of additional animals. This initiative will

help to establish reproducible data standards. Independent reanalysis of deposited data will also help identify and correct errors, prevent future experimental errors, verify data quality and in the long term, improve the replicability of experiments. Although several preclinical databases already host indirect calorimetry results for browsing and download, they often restrict data contributions from non-affiliated users[141–145]. In summary, creating a focused data repository for body weight regulation is essential for managing the rapidly growing volume of studies and promoting a deeper understanding that could lead to important biological insights and discovery.

Future-proofing

Our methods of phenotypic analysis are continuously evolving with new technological advances and understanding. For instance, mouse behaviour varies considerably between 12-hour dark and light photoperiods[146]. Traditionally, we use these cycles as our standard time blocks for analysis between groups (Fig. 3g). Our understanding of sleep, rest and activity bouts during these photoperiods, particularly concerning ultradian rhythms, is still developing[74,147]. As we gain deeper insights into these shorter time intervals and with the advent of high-resolution metabolic phenotyping, future methods could move beyond simply categorizing behaviours by dark, light and full day periods, allowing for more precise classifications. For example, body temperature changes drive a large fraction of the variation in an individual mouse's energy expenditure[74]. A repository should be compatible with additional physiological data recordings (for example, body temperature, blood levels of glucose, heart rate or other parameters). A repository should also be adaptable to encompass more complicated study designs beyond basal metabolic phenotyping between two groups. By storing and sharing our collective data, we envision a future in which additional insights will come from old experiments.

Conclusions

We conclude that the field is currently in an unsatisfactory state, with the many units used for one representative pathway (Table 1). Without standardized data analysis or visualization, comparing studies from multiple labs becomes problematic, if not impossible. As an example, we present the case of the human genes, *ACVR1C* and *INHBE*, which are associated with altered body composition. Human genetic variation in *ACVR1C* and *INHBE* is associated with differences in waist-to-hip ratio and the development of type 2 diabetes[148]. Germline whole-body knockouts of any one of the *Acvr1c*, *Inhbe* and *Gdf3* genes alter mouse body weight. Yet, the cause of the weight loss, and whether this is shared between models, is unclear owing to the different methods of analysis.

Before the printing press, standardized spelling did not exist in the English language[149]. In fact, Shakespeare's plays contain words with multiple spellings. By setting consensus standards, we aim to eliminate the use of varied units for representing metabolic rates in preclinical indirect calorimetry experiments. Although past studies might need to be repeated or reinterpreted, these earlier studies reflect the standards of their time. We would not say that Shakespeare misspelled his words, but that he practiced by the standards of his time. Dividing by body weight was the accepted standard in 2008, but our understanding has since evolved. We now know better. Similarly, post-publication peer review platforms, such as Pubpeer, should not critique the historical use of non-standard units in indirect calorimetry. Instead, we wish to move forward with new standards. Researchers choosing to not adopt these standards going forward should justify this choice and are subject to post-publication peer review by the community. Beginning in 2025, the proposed standards will apply to indirect calorimetry experiments in which there are differences in body weight or composition among animal groups of the same species. We hope this consensus guide lays the necessary groundwork for this field to grow, evolve and discover. During revision of this manuscript, two new tools have emerged that have the potential to offer new features to indirect calorimetry analysis. As they develop, it will be helpful if they can contribute in the goals to standardize analysis within the field[150,151].

References

1. Lavoisier, A. L. & Marquis de Laplace, P. S. *Mémoire sur la chaleur: Lû à'Académie royale des sciences, le 28 juin 1783*. (De l'Imprimerie royale, 1783).
2. Shechtman, O. & Talan, M. I. Effect of exercise on cold tolerance and metabolic heat production in adult and aged C57BL/6J mice. *J. Appl. Physiol.* **77**, 2214–2218 (1994).
3. Susulic, V. S. et al. Targeted disruption of the β3-adrenergic receptor gene. *J. Biol. Chem.* **270**, 29483–29492 (1995).
4. Pelleymounter, M. A. et al. Effects of the obese gene product on body weight regulation in ob/ob mice. *Science* **269**, 540–543 (1995).
5. Speakman, J. R. & McQueenie, J. Limits to sustained metabolic rate: the link between food intake, basal metabolic rate, and morphology in reproducing mice, *Mus musculus*. *Physiological Zool.* **69**, 746–769 (1996).
6. Ravussin, E., Burnand, B., Schutz, Y. & Jequier, E. Twenty-four-hour energy expenditure and resting metabolic rate in obese, moderately obese, and control subjects. *Am. J. Clin. Nutr.* **35**, 566–573 (1982).
7. Brychta, R. & Chen, K. Cold-induced thermogenesis in humans. *Eur. J. Clin. Nutr.* **71**, 345–352 (2017).
8. Achamrah, N., Delsoglio, M., De Waele, E., Berger, M. M. & Pichard, C. Indirect calorimetry: the 6 main issues. *Clin. Nutr.* **40**, 4–14 (2021).
9. Duivenvoorde, L. P., van Schothorst, E. M., Swarts, H. J. & Keijer, J. Assessment of metabolic flexibility of old and adult mice using three noninvasive, indirect calorimetry-based treatments. *J. Gerontol. A Biol. Sci. Med Sci.* **70**, 282–293 (2015).
10. Houtkooper, R. H. et al. The metabolic footprint of aging in mice. *Sci. Rep.* **1**, 134 (2011).
11. Schefer, V. & Talan, M. I. Oxygen consumption in adult and AGED C57BL/6J mice during acute treadmill exercise of different intensity. *Exp. Gerontol.* **31**, 387–392 (1996).
12. Petr, M. A. et al. A cross-sectional study of functional and metabolic changes during aging through the lifespan in male mice. *eLife* **10**, e62952 (2021).
13. Ellacott, K. L., Morton, G. J., Woods, S. C., Tso, P. & Schwartz, M. W. Assessment of feeding behavior in laboratory mice. *Cell Metab.* **12**, 10–17 (2010).
14. Martin, R. E. et al. Maternal oxycodone treatment results in neurobehavioral disruptions in mice offspring. *eNeuro* **8**, ENEURO.0150–21.2021 (2021).
15. Sanchez-Alavez, M., Bortell, N., Galmozzi, A., Conti, B. & Marcondes, M. C. G. Reactive oxygen species scavenger *N*-acetyl cysteine reduces methamphetamine-induced hyperthermia without affecting motor activity in mice. *Temperature* **1**, 227–241 (2014).
16. Rupprecht, L. E. et al. Self-administered nicotine increases fat metabolism and suppresses weight gain in male rats. *Psychopharmacology* **235**, 1131–1140 (2018).
17. Addolorato, G., Capristo, E., Greco, A., Stefanini, G. & Gasbarrini, G. Influence of chronic alcohol abuse on body weight and energy metabolism: is excess ethanol consumption a risk factor for obesity or malnutrition? *J. Intern. Med.* **244**, 387–395 (1998).
18. Levine, J. A., Harris, M. M. & Morgan, M. Y. Energy expenditure in chronic alcohol abuse. *Eur. J. Clin. Invest* **30**, 779–786 (2000).
19. Schwindinger, W. F., Borrell, B. M., Waldman, L. C. & Robishaw, J. D. Mice lacking the G protein γ3-subunit show resistance to opioids and diet induced obesity. *Am. J. Physiol. Regul. Integr. Comp. Physiol.* **297**, R1494–R1502 (2009).

20. Bonasera, S. J., Chaudoin, T. R., Goulding, E. H., Mittek, M. & Dunaevsky, A. Decreased home cage movement and oromotor impairments in adult Fmr1-KO mice. *Genes Brain Behav.* **16**, 564–573 (2017).
21. Gremminger, V. L. et al. Skeletal muscle specific mitochondrial dysfunction and altered energy metabolism in a murine model (oim/oim) of severe osteogenesis imperfecta. *Mol. Genet Metab.* **132**, 244–253 (2021).
22. Nandy, A. et al. Lipolysis supports bone formation by providing osteoblasts with endogenous fatty acid substrates to maintain bioenergetic status. *Bone Res.* **11**, 62 (2023).
23. Rossi, J. et al. Melanocortin-4 receptors expressed by cholinergic neurons regulate energy balance and glucose homeostasis. *Cell Metab.* **13**, 195–204 (2011).
24. Zhang, J., Chen, D., Sweeney, P. & Yang, Y. An excitatory ventromedial hypothalamus to paraventricular thalamus circuit that suppresses food intake. *Nat. Commun.* **11**, 6326 (2020).
25. Piñol, R. A. et al. Preoptic BRS3 neurons increase body temperature and heart rate via multiple pathways. *Cell Metab.* **33**, 1389–1403 (2021).
26. Cavalcanti-de-Albuquerque, J. P., Bober, J., Zimmer, M. R. & Dietrich, M. O. Regulation of substrate utilization and adiposity by Agrp neurons. *Nat. Commun.* **10**, 311 (2019).
27. Lerner, L. et al. MAP3K11/GDF15 axis is a critical driver of cancer cachexia. *J. Cachexia Sarcopenia Muscle* **7**, 467–482 (2016).
28. Falconer, J. S., Fearon, K. C., Plester, C. E., Ross, J. A. & Carter, D. C. Cytokines, the acute-phase response, and resting energy expenditure in cachectic patients with pancreatic cancer. *Ann. Surg.* **219**, 325–331 (1994).
29. Suriben, R. et al. Antibody-mediated inhibition of GDF15–GFRAL activity reverses cancer cachexia in mice. *Nat. Med.* **26**, 1264–1270 (2020).
30. Kliewer, K. L. et al. Adipose tissue lipolysis and energy metabolism in early cancer cachexia in mice. *Cancer Biol. Ther.* **16**, 886–897 (2015).
31. Tsoli, M. et al. Activation of thermogenesis in brown adipose tissue and dysregulated lipid metabolism associated with cancer cachexia in mice. *Cancer Res.* **72**, 4372–4382 (2012).
32. Kir, S. et al. PTH/PTHrP receptor mediates cachexia in models of kidney failure and cancer. *Cell Metab.* **23**, 315–323 (2016).
33. Desai, M. S. et al. Hypertrophic cardiomyopathy and dysregulation of cardiac energetics in a mouse model of biliary fibrosis. *Hepatology* **51**, 2097–2107 (2010).
34. Darrah, R. J. et al. Ventilatory pattern and energy expenditure are altered in cystic fibrosis mice. *J. Cyst. Fibros.* **12**, 345–351 (2013).
35. Yang, J. N., Wang, Y., Garcia-Roves, P. M., Bjornholm, M. & Fredholm, B. B. Adenosine A(3) receptors regulate heart rate, motor activity and body temperature. *Acta Physiol.* **199**, 221–230 (2010).
36. Lakin, R. et al. Changes in heart rate and its regulation by the autonomic nervous system do not differ between forced and voluntary exercise in mice. *Front. Physiol.* **9**, 841 (2018).
37. Roy, A. et al. Cardiomyocyte-secreted acetylcholine is required for maintenance of homeostasis in the heart. *FASEB J.* **27**, 5072–5082 (2013).
38. Tang, K. et al. Impaired exercise capacity and skeletal muscle function in a mouse model of pulmonary inflammation. *J. Appl. Physiol.* **114**, 1340–1350 (2013).
39. Van Remoortel, H. et al. Validity of six activity monitors in chronic obstructive pulmonary disease: a comparison with indirect calorimetry. *PloS ONE* **7**, e39198 (2012).
40. West, J. et al. A potential role for insulin resistance in experimental pulmonary hypertension. *Eur. Respir. J.* **41**, 861–871 (2013).
41. Swoap, S. J. et al. Vagal tone dominates autonomic control of mouse heart rate at thermoneutrality. *Am. J. Physiol. Heart Circ. Physiol.* **294**, H1581–H1588 (2008).
42. Lowell, B. B. & Bachman, E. S. Beta-adrenergic receptors, diet-induced thermogenesis, and obesity. *J. Biol. Chem.* **278**, 29385–29388 (2003).
43. Kazak, L. et al. A creatine-driven substrate cycle enhances energy expenditure and thermogenesis in beige fat. *Cell* **163**, 643–655 (2015).
44. Seale, P. et al. Prdm16 determines the thermogenic program of subcutaneous white adipose tissue in mice. *J. Clin. Investig.* **121**, 96–105 (2011).
45. Sass, F. et al. NK2R control of energy expenditure and feeding to treat metabolic diseases. *Nature* **635**, 987–1000 (2024).
46. Clapham, J. C. & Arch, J. R. Targeting thermogenesis and related pathways in anti-obesity drug discovery. *Pharmacol. Ther.* **131**, 295–308 (2011).
47. Baggio, L. L., Huang, Q., Brown, T. J. & Drucker, D. J. Oxyntomodulin and glucagon-like peptide-1 differentially regulate murine food intake and energy expenditure. *Gastroenterology* **127**, 546–558 (2004).
48. Schreiber, R. et al. Hypophagia and metabolic adaptations in mice with defective ATGL-mediated lipolysis cause resistance to HFD-induced obesity. *Proc. Natl Acad. Sci. USA* **112**, 13850–13855 (2015).
49. Shin, H. et al. Lipolysis in brown adipocytes is not essential for cold-induced thermogenesis in mice. *Cell Metab.* **26**, 764–777 (2017).
50. Gavrilova, O. et al. Surgical implantation of adipose tissue reverses diabetes in lipoatrophic mice. *J. Clin. Invest.* **105**, 271–278 (2000).
51. Marcaletti, S., Thomas, C. & Feige, J. N. Exercise performance tests in mice. *Curr. Protoc. Mouse Biol.* **1**, 141–154 (2011).
52. Scott, C. B. & Kemp, R. B. Direct and indirect calorimetry of lactate oxidation: implications for whole-body energy expenditure. *J. Sports Sci.* **23**, 15–19 (2005).
53. Flynn, J. M., Meadows, E., Fiorotto, M. & Klein, W. H. Myogenin regulates exercise capacity and skeletal muscle metabolism in the adult mouse. *PloS ONE* **5**, e13535 (2010).
54. Virtue, S., Even, P. & Vidal-Puig, A. Below thermoneutrality, changes in activity do not drive changes in total daily energy expenditure between groups of mice. *Cell Metab.* **16**, 665–671 (2012).
55. De Siqueira, M. K. et al. Infection-elicited microbiota promotes host adaptation to nutrient restriction. *Proc. Natl Acad. Sci. USA* **120**, e2214484120 (2023).
56. van der Zande, H. J. P. et al. The helminth glycoprotein omega-1 improves metabolic homeostasis in obese mice through type 2 immunity-independent inhibition of food intake. *FASEB J.* **35**, e21331 (2021).
57. Nolan, K. E. et al. Metabolic shifts modulate lung injury caused by infection with H1N1 influenza A virus. *Virology* **559**, 111–119 (2021).
58. Melchor, S. J. et al. *T. gondii* infection induces IL-1R dependent chronic cachexia and perivascular fibrosis in the liver and skeletal muscle. *Sci. Rep.* **10**, 15724 (2020).
59. Kohlgruber, A. C. et al. γΔ T cells producing interleukin-17A regulate adipose regulatory T cell homeostasis and thermogenesis. *Nat. Immunol.* **19**, 464–474 (2018).
60. Hu, B. et al. γΔ T cells and adipocyte IL-17RC control fat innervation and thermogenesis. *Nature* **578**, 610–614 (2020).
61. Kong, X. et al. IRF4 is a key thermogenic transcriptional partner of PGC-1α. *Cell* **158**, 69–83 (2014).
62. Lai, N., Kummitha, C., Drumm, M. & Hoppel, C. Alterations of skeletal muscle bioenergetics in a mouse with F508del mutation leading to a cystic fibrosis-like condition. *Am. J. Physiol.-Endocrinol. Metab.* **317**, E327–E336 (2019).

63. Pant, M. et al. Metabolic dysfunction and altered mitochondrial dynamics in the utrophin-dystrophin deficient mouse model of duchenne muscular dystrophy. *PloS ONE* **10**, e0123875 (2015).
64. Rocco, A. B., Levalley, J. C., Eldridge, J. A., Marsh, S. A. & Rodgers, B. D. A novel protocol for assessing exercise performance and dystropathophysiology in the mdx mouse. *Muscle Nerve* **50**, 541–548 (2014).
65. Maricelli, J. W. et al. Sexually dimorphic skeletal muscle and cardiac dysfunction in a mouse model of limb girdle muscular dystrophy 2i. *J. Appl. Physiol.* **123**, 1126–1138 (2017).
66. Meng, X. et al. Manipulations of MeCP2 in glutamatergic neurons highlight their contributions to Rett and other neurological disorders. *eLife* **5**, e14199 (2016).
67. Stojakovic, A. et al. Partial inhibition of mitochondrial complex I ameliorates Alzheimer's disease pathology and cognition in APP/PS1 female mice. *Commun. Biol.* **4**, 61 (2021).
68. Dufour, B. D. & McBride, J. L. Normalizing glucocorticoid levels attenuates metabolic and neuropathological symptoms in the R6/2 mouse model of Huntington's disease. *Neurobiol. Dis.* **121**, 214–229 (2019).
69. Speakman, J. R., Selman, C., McLaren, J. S. & Harper, E. J. Living fast, dying when? The link between aging and energetics. *J. Nutr.* **132**, 1583S–1597S (2002).
70. Nicholls, H. T., Krisko, T. I., LeClair, K. B., Banks, A. S. & Cohen, D. E. Regulation of adaptive thermogenesis by the gut microbiome. *FASEB J.* **30**, 854.852 (2016).
71. López, P. et al. Long-term genistein consumption modifies gut microbiota, improving glucose metabolism, metabolic endotoxemia, and cognitive function in mice fed a high-fat diet. *Mol. Nutr. Food Res.* **62**, 1800313 (2018).
72. Sharma, V. et al. Mannose alters gut microbiome, prevents diet-induced obesity, and improves host metabolism. *Cell Rep.* **24**, 3087–3098 (2018).
73. Hansotia, T. et al. Extrapancreatic incretin receptors modulate glucose homeostasis, body weight, and energy expenditure. *J. Clin. Invest* **117**, 143–152 (2007).
74. Škop, V. et al. Beyond day and night: the importance of ultradian rhythms in mouse physiology. *Mol. Metab.* **84**, 101946 (2024).
75. Brager, A. J. et al. Homeostatic effects of exercise and sleep on metabolic processes in mice with an overexpressed skeletal muscle clock. *Biochimie* **132**, 161–165 (2017).
76. Yajima, K. et al. Effects of nutrient composition of dinner on sleep architecture and energy metabolism during sleep. *J. Nutr. Sci. Vitaminol.* **60**, 114–121 (2014).
77. Wang, Y. et al. Chronic sleep fragmentation promotes obesity in young adult mice. *Obesity* **22**, 758–762 (2014).
78. Nestoridi, E., Kvas, S., Kucharczyk, J. & Stylopoulos, N. Resting energy expenditure and energetic cost of feeding are augmented after Roux-en-Y gastric bypass in obese mice. *Endocrinology* **153**, 2234–2244 (2012).
79. Harris, D. A. et al. Sleeve gastrectomy enhances glucose utilization and remodels adipose tissue independent of weight loss. *Am. J. Physiol. Endocrinol. Metab.* **318**, E678–E688 (2020).
80. Tran, T. T., Yamamoto, Y., Gesta, S. & Kahn, C. R. Beneficial effects of subcutaneous fat transplantation on metabolism. *Cell Metab.* **7**, 410–420 (2008).
81. McLean, J. & Tobin, G. *Animal and Human Calorimetry* (Cambridge University Press, 1987).
82. Gavrilova, O. et al. Torpor in mice is induced by both leptin-dependent and-independent mechanisms. *Proc. Natl Acad. Sci. USA* **96**, 14623–14628 (1999).
83. Gilbert, R. E. et al. SIRT1 activation ameliorates hyperglycaemia by inducing a torpor-like state in an obese mouse model of type 2 diabetes. *Diabetologia* **58**, 819–827 (2015).
84. Wahlang, B. et al. A compromised liver alters polychlorinated biphenyl-mediated toxicity. *Toxicology* **380**, 11–22 (2017).
85. Somani, S. M., Husain, K., Asha, T. & Helfert, R. Interactive and delayed effects of pyridostigmine and physical stress on biochemical and histological changes in peripheral tissues of mice. *J. Appl. Toxicol.* **20**, 327–334 (2000).
86. Field, D. et al. The Genomic Standards Consortium. *PLoS Biol.* **9**, e1001088 (2011).
87. Alseekh, S. et al. Mass spectrometry-based metabolomics: a guide for annotation, quantification and best reporting practices. *Nat. Methods* **18**, 747–756 (2021).
88. Even, P. C. & Nadkarni, N. A. Indirect calorimetry in laboratory mice and rats: principles, practical considerations, interpretation and perspectives. *Am. J. Physiol. Regul. Integr. Comp. Physiol.* **303**, R459–476 (2012).
89. Kleiber, M. Body size and metabolism. *Hilgardia* **6**, 315–353 (1932).
90. White, C. R. & Seymour, R. S. Allometric scaling of mammalian metabolism. *J. Exp. Biol.* **208**, 1611–1619 (2005).
91. Heusner, A. A. Size and power in mammals. *J. Exp. Biol.* **160**, 25–54 (1991).
92. Speakman, J. R. et al. The international atomic energy agency international doubly labelled water database: aims, scope and procedures. *Ann. Nutr. Metab.* **75**, 114–118 (2019).
93. Pontzer, H. et al. Daily energy expenditure through the human life course. *Science* **373**, 808–812 (2021).
94. McPherron, A. C. & Lee, S.-J. Suppression of body fat accumulation in myostatin-deficient mice. *J. Clin. Investig.* **109**, 595–601 (2002).
95. Westbrook, R., Bonkowski, M. S., Strader, A. D. & Bartke, A. Alterations in oxygen consumption, respiratory quotient, and heat production in long-lived GHRKO and Ames dwarf mice, and short-lived bGH transgenic mice. *J. Gerontol. A Biol. Sci. Med Sci.* **64**, 443–451 (2009).
96. Longo, K. A. et al. Daily energy balance in growth hormone receptor/binding protein ($GHR^{-/-}$) gene-disrupted mice is achieved through an increase in dark-phase energy efficiency. *Growth Horm. IGF Res.* **20**, 73–79 (2010).
97. Meyer, C. W., Klingenspor, M., Rozman, J. & Heldmaier, G. Gene or size: metabolic rate and body temperature in obese growth hormone-deficient dwarf mice. *Obes. Res.* **12**, 1509–1518 (2004).
98. Himms-Hagen, J. On raising energy expenditure in ob/ob mice. *Science* **276**, 1132–1133 (1997).
99. Krashes, M. J., Lowell, B. B. & Garfield, A. S. Melanocortin-4 receptor-regulated energy homeostasis. *Nat. Neurosci.* **19**, 206–219 (2016).
100. Rajbhandari, P. et al. IL-10 signaling remodels adipose chromatin architecture to limit thermogenesis and energy expenditure. *Cell* **172**, 218–233 (2018).
101. Westbrook, R. M. et al. Aged interleukin-10tm1Cgn chronically inflamed mice have substantially reduced fat mass, metabolic rate, and adipokines. *PloS ONE* **12**, e0186811 (2017).
102. Mina, A. I. et al. CalR: a web-based analysis tool for indirect calorimetry experiments. *Cell Metab.* **28**, 656–666 (2018).
103. El-Haschimi, K., Pierroz, D. D., Hileman, S. M., Bjørbæk, C. & Flier, J. S. Two defects contribute to hypothalamic leptin resistance in mice with diet-induced obesity. *J. Clin. Investig.* **105**, 1827–1832 (2000).
104. Corrigan, J. K. et al. A big-data approach to understanding metabolic rate and response to obesity in laboratory mice. *eLife* **9**, e53560 (2020).
105. Taicher, G. Z., Tinsley, F. C., Reiderman, A. & Heiman, M. L. Quantitative magnetic resonance (QMR) method for bone and whole-body-composition analysis. *Anal. Bioanal. Chem.* **377**, 990–1002 (2003).

106. Packard, G. C. & Boardman, T. J. The use of percentages and size-specific indices to normalize physiological data for variation in body size: wasted time, wasted effort? *Comp. Biochem. Physiol. A Mol. Integr. Physiol.* **122**, 37–44 (1999).
107. Grobe, J. L. in *The Renin-Angiotensin-Aldosterone System: Methods and Protocols* (ed Sean E. Thatcher) 123–146 (Springer, 2017).
108. Kaiyala, K. J. & Schwartz, M. W. Toward a more complete (and less controversial) understanding of energy expenditure and its role in obesity pathogenesis. *Diabetes* **60**, 17–23 (2011).
109. Licholai, J. A. et al. Why do mice overeat high-fat diets? How high-fat diet alters the regulation of daily caloric intake in mice. *Obesity* **26**, 1026–1033 (2018).
110. Rubio, W. B., Cortopassi, M. D. & Banks, A. S. Indirect calorimetry to assess energy balance in mice: measurement and data analysis. *Methods Mol. Biol.* **2662**, 103–115 (2023).
111. Rubio, W. B. et al. Not so fast: paradoxically increased variability in the glucose tolerance test due to food withdrawal in continuous glucose-monitored mice. *Mol. Metab.* **77**, 101795 (2023).
112. Schipper, L. et al. Grain versus AIN: common rodent diets differentially affect health outcomes in adult C57BL/6j mice. *PloS ONE* **19**, e0293487 (2024).
113. Glendinning, J. I. et al. Differential effects of sucrose and fructose on dietary obesity in four mouse strains. *Physiol. Behav.* **101**, 331–343 (2010).
114. Kim, A. K., Hamadani, C., Zeidel, M. L. & Hill, W. G. Urological complications of obesity and diabetes in males and females of three mouse models: temporal manifestations. *Am. J. Physiol. Ren. Physiol.* **318**, F160–F174 (2020).
115. Bertaggia, E. et al. Cyp8b1 ablation prevents Western diet-induced weight gain and hepatic steatosis because of impaired fat absorption. *Am. J. Physiol. Endocrinol. Metab.* **313**, E121–E133 (2017).
116. Weir, J. B. New methods for calculating metabolic rate with special reference to protein metabolism. *J. Physiol.* **109**, 1–9 (1949).
117. Lighton, J. R. B. *Measuring Metabolic Rates: A Manual for Scientists*. (Oxford University Press, 2019).
118. Raubenheimer, D. & Simpson, S. Analysis of covariance: an alternative to nutritional indices. *Entomol. Exp. Appl.* **62**, 221–231 (1992).
119. Kronmal, R. A. Spurious correlation and the fallacy of the ratio standard revisited. *J. R. Stat. Soc.* **156**, 379–392 (1993).
120. Albrecht, G. H., Gelvin, B. R. & Hartman, S. E. Ratios as a size adjustment in morphometrics. *Am. J. Phys. Anthropol.* **91**, 441–468 (1993).
121. Allison, D., Paultre, F., Goran, M., Poehlman, E. & Heymsfield, S. Statistical considerations regarding the use of ratios to adjust data. *Int. J. Obes. Relat. Metab. Disord.* **19**, 644–652 (1995).
122. Raubenheimer, D. Problems with ratio analysis in nutritional studies. *Funct. Ecol.* **9**, 21–29 (1995).
123. Speakman, J. R., Fletcher, Q. & Vaanholt, L. The '39 steps': an algorithm for performing statistical analysis of data on energy intake and expenditure. *Dis. Model. Mech.* **6**, 293–301 (2013).
124. Arch, J., Hislop, D., Wang, S. & Speakman, J. Some mathematical and technical issues in the measurement and interpretation of open-circuit indirect calorimetry in small animals. *Int. J. Obes.* **30**, 1322–1331 (2006).
125. Packard, G. C. & Boardman, T. J. The misuse of ratios, indices, and percentages in ecophysiological research. *Physiol. Zool.* **61**, 1–9 (1988).
126. Kaiyala, K. J. et al. Identification of body fat mass as a major determinant of metabolic rate in mice. *Diabetes* **59**, 1657–1666 (2010).
127. Kaiyala, K. J. Mathematical model for the contribution of individual organs to non-zero y-intercepts in single and multi-compartment linear models of whole-body energy expenditure. *PloS ONE* **9**, e103301 (2014).
128. Poehlman, E. T. & Toth, M. J. Mathematical ratios lead to spurious conclusions regarding age-and sex-related differences in resting metabolic rate. *Am. J. Clin. Nutr.* **61**, 482–485 (1995).
129. Tschöp, M. H. et al. A guide to analysis of mouse energy metabolism. *Nat. Methods* **9**, 57–63 (2012).
130. Fernandez-Verdejo, R., Ravussin, E., Speakman, J. R. & Galgani, J. E. Progress and challenges in analyzing rodent energy expenditure. *Nat. Methods* **16**, 797–799 (2019).
131. Muller, T. D., Klingenspor, M. & Tschop, M. H. Revisiting energy expenditure: how to correct mouse metabolic rate for body mass. *Nat. Metab.* **3**, 1134–1136 (2021).
132. D'Alonzo, K. T. The Johnson–Neyman procedure as an alternative to ANCOVA. *West. J. Nurs. Res.* **26**, 804–812 (2004).
133. Toyama, K. S. J. Nplots: an R package to visualize outputs from the Johnson–Neyman technique for categorical and continuous moderators, including options for phylogenetic regressions. *Evolut. Ecol.* **38**, 371–385 (2024).
134. Virtue, S., Lelliott, C. J. & Vidal-Puig, A. What is the most appropriate covariate in ANCOVA when analysing metabolic rate? *Nat. Metab.* **3**, 1585–1585 (2021).
135. Selman, C., Lumsden, S., Bünger, L., Hill, W. G. & Speakman, J. R. Resting metabolic rate and morphology in mice (*Mus musculus*) selected for high and low food intake. *J. Exp. Biol.* **204**, 777–784 (2001).
136. Drucker, D. J. Never waste a good crisis: confronting reproducibility in translational research. *Cell Metab.* **24**, 348–360 (2016).
137. Cobey, K. D. et al. Biomedical researchers' perspectives on the reproducibility of research. *PLoS Biol.* **22**, e3002870 (2024).
138. Sciences, N. A. o. et al. *Reproducibility and Replicability in Science*. (National Academies Press, 2019).
139. Gabelica, M., Bojčić, R. & Puljak, L. Many researchers were not compliant with their published data sharing statement: a mixed-methods study. *J. Clin. Epidemiol.* **150**, 33–41 (2022).
140. Wilkinson, M. D. et al. The FAIR Guiding Principles for scientific data management and stewardship. *Sci. Data* **3**, 160018 (2016).
141. Rozman, J. et al. Identification of genetic elements in metabolism by high-throughput mouse phenotyping. *Nat. Commun.* **9**, 288 (2018).
142. Gailus-Durner, V. et al. Introducing the German Mouse Clinic: open access platform for standardized phenotyping. *Nat. Methods* **2**, 403–404 (2005).
143. Bogue, M. A., Churchill, G. A. & Chesler, E. J. Collaborative cross and diversity outbred data resources in the mouse phenome database. *Mamm. Genome* **26**, 511–520 (2015).
144. Ayala, J. E. et al. Standard operating procedures for describing and performing metabolic tests of glucose homeostasis in mice. *Dis. Model. Mech.* **3**, 525–534 (2010).
145. Bachmann, A. M. et al. Genetic background and sex control the outcome of high-fat diet feeding in mice. *iScience* **25**, 104468 (2022).
146. Vitaterna, M. H. et al. Mutagenesis and mapping of a mouse gene, *Clock*, essential for circadian behavior. *Science* **264**, 719–725 (1994).
147. Blessing, W. & Ootsuka, Y. Timing of activities of daily life is jaggy: how episodic ultradian changes in body and brain temperature are integrated into this process. *Temperature* **3**, 371–383 (2016).
148. Deaton, A. M. et al. Rare loss of function variants in the hepatokine gene INHBE protect from abdominal obesity. *Nat. Commun.* **13**, 4319 (2022).

149. Howard-Hill, T. H. Early modern printers and the standardization of english spelling. *Mod. Lang. Rev.* **101**, 16–29 (2006).
150. Loipfinger, S. et al. Calopy — an advanced framework for the integration and analysis of indirect calorimetry data. *Nat. Metab.* **7**, 1093–1095 (2025).
151. Grein, S. et al. Shiny-Calorie: a context-aware application for indirect calorimetry data analysis and visualization using R. Preprint at *bioRxiv* https://doi.org/10.1101/2025.04.24.648116 (2025).
152. Hashimoto, O. et al. Activin E controls energy homeostasis in both brown and white adipose tissues as a hepatokine. *Cell Rep.* **25**, 1193–1203 (2018).
153. Koncarevic, A. et al. A novel therapeutic approach to treating obesity through modulation of TGFβ signaling. *Endocrinology* **153**, 3133–3146 (2012).
154. Yadav, H. et al. Protection from obesity and diabetes by blockade of TGF-β/Smad3 signaling. *Cell Metab.* **14**, 67–79 (2011).
155. Wilkes, J. J., Lloyd, D. J. & Gekakis, N. Loss-of-function mutation in myostatin reduces tumor necrosis factor α production and protects liver against obesity-induced insulin resistance. *Diabetes* **58**, 1133–1143 (2009).
156. Shen, J. J. et al. Deficiency of growth differentiation factor 3 protects against diet-induced obesity by selectively acting on white adipose. *Mol. Endocrinol.* **23**, 113–123 (2009).
157. Yogosawa, S., Mizutani, S., Ogawa, Y. & Izumi, T. Activin receptor-like kinase 7 suppresses lipolysis to accumulate fat in obesity through downregulation of peroxisome proliferator-activated receptor gamma and C/EBPalpha. *Diabetes* **62**, 115–123 (2013).
158. Tangseefa, P., Jin, H., Zhang, H., Xie, M. & Ibáñez, C. F. Human ACVR1C missense variants that correlate with altered body fat distribution produce metabolic alterations of graded severity in knock-in mutant mice. *Mol. Metab.* **81**, 101890 (2024).
159. Kumari, R. *Role of SMAD2 and SMAD3 on Adipose Tissue Development and Function*. (The University of Tennessee Health Science Center, 2021).
160. Kumari, R. et al. SMAD2 and SMAD3 differentially regulate adiposity and the growth of subcutaneous white adipose tissue. *FASEB J.* **35**, e22018 (2021).
161. Zhao, M. et al. Targeting activin receptor–like kinase 7 ameliorates adiposity and associated metabolic disorders. *JCI Insight* **8**, e161229 (2023).
162. Srivastava, R. K., Lee, E. S., Sim, E., Sheng, N. C. & Ibáñez, C. F. Sustained anti-obesity effects of life-style change and anti-inflammatory interventions after conditional inactivation of the activin receptor ALK7. *FASEB J.* **35**, e21759 (2021).
163. Guo, T. et al. Adipocyte ALK7 links nutrient overload to catecholamine resistance in obesity. *eLife* **3**, e03245 (2014).
164. Choi, S. J. et al. Increased energy expenditure and leptin sensitivity account for low fat mass in myostatin-deficient mice. *Am. J. Physiol. Endocrinol. Metab.* **300**, E1031–E1037 (2011).
165. Wang, H. et al. Myostatin regulates energy homeostasis through autocrine- and paracrine-mediated microenvironment communication. *J. Clin. Invest.* **134**, e178303 (2024).
166. Akpan, I. et al. The effects of a soluble activin type IIB receptor on obesity and insulin sensitivity. *Int. J. Obes.* **33**, 1265–1273 (2009).
167. Abreu-Vieira, G., Xiao, C., Gavrilova, O. & Reitman, M. L. Integration of body temperature into the analysis of energy expenditure in the mouse. *Mol. Metab.* **4**, 461–470 (2015).
168. Percie du Sert, N. et al. The ARRIVE guidelines 2.0: updated guidelines for reporting animal research. *PLoS Biol.* **18**, e3000410 (2020).

Acknowledgements

Funding is provided by NIH grants R01DK133948 and P30DK135043 (A.S.B.), P30DK056350 (S.R.S.), U2CDK135074 (K.L.), U2CDK135073 (J.A. and L.L.), U2CDK135066 (C.E.), U2CDK134901 (G.S.) and FAPESP grant #2013/07607-8 (L.A.V.).

Author contributions

In hopes of creating a set of global standards for preclinical indirect calorimetry experiments, we assembled the International Indirect Calorimetry Consensus Committee (IICCC). The initial composition includes 79 members in 18 countries. The effort and initial draft grew from the NIH-funded Mouse Metabolic Phenotyping Centers Reproducibility Working Group. Input was then solicited from calorimetry leaders within the NIDDK-Diabetes Research Centers, NIDDK-Nutrition Obesity Research Centers, International Mouse Phenotyping Consortium and additional experts at independent sites. All members enthusiastically support the need for greater standards in indirect calorimetry research and will continue to actively promote and maintain these standards. A draft of the guide was shared by the IICCC chair (A.S.B.). Written comments and suggestions from committee members were received, including revision assistance by C.D.H. Virtual discussion meetings were held. The submitted manuscript reflects changes from these discussions, editorial suggestions from *Nature Metabolism* and peer reviewers.

Competing interests

M.D., K.S. and J.R.Z. organized an indirect calorimetry course, and travel was provided to C.D.H. as an indirect calorimetry course guest lecturer by Sable Systems International. J.R.S. consults for TSE International. The remaining authors declare no competing interests.

Additional information

Correspondence and requests for materials should be addressed to Alexander S. Banks.

Peer review information *Nature Metabolism* thanks Dominik Lutter, Jae Myoung Suh and the other, anonymous, reviewer(s) for their contribution to the peer review of this work. Primary Handling Editor: Alfredo Giménez-Cassina, in collaboration with the *Nature Metabolism* team.

https://doi.org/10.1038/s42255-025-01360-4

Alexander S. Banks[1] ✉, David B. Allison[2], Thierry Alquier[3,4], Ansarullah[5], Steven N. Austad[6,7], Johan Auwerx[8], Julio E. Ayala[9,10], Joseph A. Baur[11,12], Stefania Carobbio[13], Gary A. Churchill[5], Morten Dall[14], Rafael de Cabo[15], Jose Donato Jr.[16], Nathalia R. V. Dragano[17,18], Carol F. Elias[19,20], Anthony W. Ferrante Jr.[21], Brian N. Finck[22], Jose E. Galgani[23,24], Zachary Gerhart-Hines[14], Laurie J. Goodyear[25], Justin L. Grobe[26,27,28,29], Rana K. Gupta[30], Kirk M. Habegger[31], Sean M. Hartig[32,33,34], Andrea L. Hevener[35,36], Steven B. Heymsfield[37], Corey D. Holman[38], Martin Hrabě de Angelis[17,18], David E. James[39,40,41], Lawrence Kazak[42,43], Jae Bum Kim[44], Martin Klingenspor[45], Xingxing Kong[46], Sander Kooijman[47,48], Louise Lantier[9,10], K. C. Kent Lloyd[49,50], James C. Lo[51,52,53], Irfan J. Lodhi[54], Paul S. MacLean[55], Owen P. McGuinness[10], Gema Medina-Gómez[56], Raghavendra G. Mirmira[57], Christopher D. Morrison[58], Gregory J. Morton[59], Timo D. Müller[60,61], Yoshihiro Ogawa[62], David Pajuelo-Reguera[63], Matthew J. Potthoff[64,65], Nathan Qi[19], Marc L. Reitman[66], Patrick C. N. Rensen[47,48], Jan Rozman[67], Jennifer M. Rutkowsky[68], Kei Sakamoto[14], Philipp E. Scherer[69], Gary J. Schwartz[70,71], Radislav Sedlacek[63], Mohammed Selloum[72], Saame Raza Shaikh[73], Shuai Chen[74,75], Gerald I. Shulman[76], Vojtěch Škop[77,78], Alexander A. Soukas[79,80], John R. Speakman[81,82,83,84], Bruce M. Spiegelman[85,86], Gregory R. Steinberg[87,88], Katrin J. Svensson[89,90,91], John P. Thyfault[92,93,94], Tony Tiganis[95,96], Paul M. Titchenell[11,12], Nigel Turner[97,98], Licio A. Velloso[99], Antonio Vidal-Puig[100,101,102,103], Christopher S. Ward[104], Ashley S. Williams[30], Christian Wolfrum[105], Allison W. Xu[106,107], Ying Xu[108] & Juleen R. Zierath[14,109,110] on behalf of The International Indirect Calorimetry Consensus Committee (IICCC)*

[1]Division of Endocrinology, Diabetes, and Metabolism, Beth Israel Deaconess Medical Center and Harvard Medical School, Boston, MA, USA. [2]Department of Epidemiology and Biostatistics, School of Public Health, Indiana University Bloomington, Bloomington, IN, USA. [3]Centre de Recherche du Centre Hospitalier de l'Université de Montréal (CRCHUM), Montreal, Quebec, Canada. [4]Department of Medicine, Université de Montréal, Montreal, Quebec, Canada. [5]The Jackson Laboratory, Bar Harbor, ME, USA. [6]Department of Biology, University of Alabama at Birmingham, Birmingham, AL, USA. [7]American Federation for Aging Research, New York, NY, USA. [8]Laboratory of Integrative Systems Physiology, Institute of Bioengineering, École Polytechnique Fédérale de Lausanne, Lausanne, Switzerland. [9]Department of Molecular Physiology and Biophysics, Vanderbilt University School of Medicine, Nashville, TN, USA. [10]Vanderbilt Mouse Metabolic Phenotyping Center, Vanderbilt University, Nashville, TN, USA. [11]Department of Physiology, Perelman School of Medicine, University of Pennsylvania, Philadelphia, PA, USA. [12]Institute for Diabetes, Obesity, and Metabolism, Perelman School of Medicine, University of Pennsylvania, Philadelphia, PA, USA. [13]Centro de Investigación Principe Felipe, Valencia, Spain. [14]Novo Nordisk Foundation Center for Basic Metabolic Research, University of Copenhagen, Copenhagen, Denmark. [15]Translational Gerontology Branch, National Institute on Aging, NIH, Baltimore, MD, USA. [16]Department of Physiology and Biophysics, Institute of Biomedical Sciences, University of São Paulo, São Paulo, Brazil. [17]Institute of Experimental Genetics - German Mouse Clinic, Helmholtz Zentrum, Munich, Germany. [18]German Center for Diabetes Research (DZD), Neuherberg, Germany. [19]Department of Molecular & Integrative Physiology, University of Michigan, Ann Arbor, MI, USA. [20]Department of Obstetrics & Gynecology, University of Michigan, Ann Arbor, MI, USA. [21]Department of Medicine, Institute of Human Nutrition, Naomi Berrie Diabetes Center, Columbia University, New York, NY, USA. [22]Center for Human Nutrition, Division of Nutritional Sciences and Obesity Medicine, Washington University School of Medicine, St Louis, MO, USA. [23]Departamento de Nutrición y Dietética, Escuela de Ciencias de la Salud, Facultad de Medicina, Pontificia Universidad Católica de Chile, Santiago, Chile. [24]Departamento de Nutrición, Diabetes y Metabolismo, Facultad de Medicina, Pontificia Universidad Católica de Chile, Santiago, Chile. [25]Section on Integrative Physiology and Metabolism, Joslin Diabetes Center, Harvard Medical School, Boston, MA, USA. [26]Department of Physiology, Medical College of Wisconsin, Milwaukee, WI, USA. [27]Department of Biomedical Engineering, Medical College of Wisconsin, Milwaukee, WI, USA. [28]Cardiovascular Center, Medical College of Wisconsin, Milwaukee, WI, USA. [29]Comprehensive Rodent Metabolic Phenotyping Core, Medical College of Wisconsin, Milwaukee, WI, USA. [30]Division of Endocrinology, Department of Medicine, Duke Molecular Physiology Institute, Duke University, Durham, NC, USA. [31]Department of Medicine, Division of Endocrinology, Diabetes & Metabolism, University of Alabama at Birmingham, Birmingham, AL, USA. [32]Department of Molecular and Cellular Biology, Baylor College of Medicine, Houston, TX, USA. [33]Department of Medicine, Baylor College of Medicine, Houston, TX, USA. [34]Division of Diabetes, Endocrinology and Metabolism, Baylor College of Medicine, Houston, TX, USA. [35]Division of Endocrinology, Diabetes and Metabolism, Department of Medicine, University of California, Los Angeles, CA, USA. [36]VA Greater Los Angeles Healthcare System GRECC, Los Angeles, CA, USA. [37]Pennington Biomedical Research Center, Louisiana State University, Baton Rouge, LA, USA. [38]Institute for Diabetes, Obesity and Metabolism, Perelman School of Medicine, University of Pennsylvania, Philadelphia, PA, USA. [39]The Charles Perkins Centre, The University of Sydney, Sydney, New South Wales, Australia. [40]School of Life and Environmental Sciences, The University of Sydney, Sydney, New South Wales, Australia. [41]School of Medical Sciences, The University of Sydney, Sydney, New South Wales, Australia. [42]Rosalind & Morris Goodman Cancer Institute, McGill University, Montreal, Quebec, Canada. [43]Department of Biochemistry, McGill University, Montreal, Quebec, Canada. [44]Center for Adipocyte Structure and Function, Institute of Molecular Biology and Genetics, School of Biological Sciences, Seoul National University, Seoul, Republic of Korea. [45]School of Life Sciences, Else Kröner Fresenius Center for Nutritional Medicine, ZIEL Institute for Food & Health, Technical University of Munich, Freising, Germany. [46]School of Life Sciences, Fudan University, Shanghai, China. [47]Division of Endocrinology, Department of Medicine, Leiden University Medical Center, Leiden, The Netherlands. [48]Einthoven Laboratory for Experimental Vascular Medicine, Leiden University Medical Center, Leiden, The Netherlands. [49]Department of Surgery, School of Medicine, University of California, Davis, Davis, CA, USA. [50]Mouse Biology Program, University of California, Davis, Davis, CA, USA. [51]Weill Center for Metabolic Health, Weill Cornell Medicine, New York, NY, USA. [52]Cardiovascular Research Institute, Weill Cornell Medicine, New York, NY, USA. [53]Division of Cardiology, Department of Medicine, Weill Cornell Medicine, New York, NY, USA. [54]Division of Endocrinology, Metabolism & Lipid Research, Department of Medicine, Washington University School of Medicine, Saint Louis, MO, USA. [55]Division of Endocrinology, Metabolism, and Diabetes, School of Medicine, University of Colorado Anschutz Medical Campus, Colorado, CO, USA. [56]Área de Bioquímica y Biología Molecular, Departamento de Ciencias Básicas de la Salud, Facultad de Ciencias de la Salud, Universidad Rey Juan Carlos, Madrid, Spain. [57]Department of Medicine, The University of Chicago, Chicago, IL, USA. [58]Pennington Biomedical Research Center, LSU System, Baton Rouge, LA, USA. [59]University of Washington Medicine Diabetes Institute, Department of Medicine, Seattle, WA, USA. [60]Institute for Diabetes and Obesity, Helmholtz Munich, Munich, Germany. [61]Walther-Straub Institute for Pharmacology and Toxicology, Ludwig-Maximilians-University Munich, Munich, Germany. [62]Department of Medicine and Bioregulatory Science, Graduate School of Medical Sciences, Kyushu University, Fukuoka, Japan. [63]Czech Centre for Phenogenomics, Institute of Molecular Genetics of the Czech Academy of Sciences, Vestec, Czechia. [64]Harold Hamm Diabetes Center, University of Oklahoma Health Sciences, Oklahoma City, OK, USA. [65]Department

of Biochemistry and Physiology, University of Oklahoma Health Sciences, Oklahoma City, OK, USA. [66]Diabetes, Endocrinology, and Obesity Branch, National Institute of Diabetes and Digestive and Kidney Diseases, NIH, Bethesda, MD, USA. [67]Luxembourg Centre for Systems Biomedicine, University of Luxembourg, Luxembourg, Luxembourg. [68]Department of Molecular Biosciences, University of California, Davis, Davis, CA, USA. [69]Touchstone Diabetes Center, University of Texas Southwestern Medical Center, Dallas, TX, USA. [70]Department of Medicine, Albert Einstein College of Medicine, Bronx, NY, USA. [71]Department of Neuroscience, Albert Einstein College of Medicine, Bronx, NY, USA. [72]Université de Strasbourg, CNRS, INSERM, CELPHEDIA, PHENOMIN, Institut Clinique de la Souris, Illkirch, France. [73]Department of Nutrition, Gillings School of Global Public Health and School of Medicine, University of North Carolina at Chapel Hill, Chapel Hill, NC, USA. [74]State Key Laboratory of Pharmaceutical Biotechnology, Model Animal Research Center, Medical School, Nanjing University, Nanjing, China. [75]Ministry of Education Key Laboratory of Model Animal for Disease Study, Model Animal Research Center, Medical School, Nanjing University, Nanjing, China. [76]Department of Cellular & Molecular Physiology, Yale School of Medicine, New Haven, CT, USA. [77]Department of Biochemistry and Microbiology, University of Chemistry and Technology, Prague, Czechia. [78]Centre for Experimental Medicine, Institute for Clinical and Experimental Medicine, Prague, Czechia. [79]Center for Genomic Medicine, Massachusetts General Hospital, Harvard Medical School, Boston, MA, USA. [80]Broad Institute of Harvard and MIT, Cambridge, MA, USA. [81]School of Biological Sciences, University of Aberdeen, Aberdeen, UK. [82]Shenzhen Key Laboratory of Metabolic Health, Center for Energy Metabolism and Reproduction, Shenzhen Institute of Advanced Technology, Chinese Academy of Sciences, Shenzhen, China. [83]Institute of Genetics and Developmental Biology, Chinese Academy of Sciences, Beijing, China. [84]Institute of Health Sciences, China Medical University, Shenyang, China. [85]Department of Cancer Biology, Dana-Farber Cancer Institute, Boston, MA, USA. [86]Department of Cell Biology, Harvard University Medical School, Boston, MA, USA. [87]Centre for Metabolism, Obesity and Diabetes Research, McMaster University, Hamilton, Ontario, Canada. [88]Division of Endocrinology and Metabolism, Department of Medicine, McMaster University, Hamilton, Ontario, Canada. [89]Department of Pathology, Stanford University School of Medicine, Stanford, CA, USA. [90]Stanford Diabetes Research Center, Stanford University School of Medicine, Stanford, CA, USA. [91]Stanford Cardiovascular Institute, Stanford University School of Medicine, Stanford, CA, USA. [92]Department of Cell Biology and Physiology, University of Kansas Medical Center, Kansas City, KS, USA. [93]Department of Internal Medicine, Division of Endocrinology, University of Kansas Medical Center, Kansas City, KS, USA. [94]KU Diabetes Institute, Kansas City, KS, USA. [95]Monash Biomedicine Discovery Institute, Monash University, Clayton, Victoria, Australia. [96]Department of Biochemistry and Molecular Biology, Monash University, Clayton, Victoria, Australia. [97]Victor Chang Cardiac Research Institute, Darlinghurst, New South Wales, Australia. [98]Faculty of Medicine and Health, UNSW Sydney, Sydney, New South Wales, Australia. [99]Obesity and Comorbidities Research Center, University of Campinas, Campinas, Brazil. [100]MRC Institute of Metabolic Science and Medical Research Council, Cambridge, UK. [101]Cambridge University Nanjing Centre of Technology and Innovation, Nanjing, PR China. [102]Centro de Investigacion Principe Felipe (CIPF), Valencia, Spain. [103]Cambridge Heart and Lung Research Institute, Cambridge, UK. [104]Department of Integrative Physiology, Baylor College of Medicine, Houston, TX, USA. [105]Department of Health Sciences and Technology, ETH Zurich, Zurich, Switzerland. [106]Diabetes Center, University of California, San Francisco, San Francisco, CA, USA. [107]Department of Anatomy, University of California, San Francisco, San Francisco, CA, USA. [108]Cambridge-Su Genomic Resource Center, The Fourth Affiliated Hospital, Medical School of Soochow University, Suzhou, China. [109]Section of Integrative Physiology, Department of Molecular Medicine and Surgery, Karolinska Institutet, Stockholm, Sweden. [110]Section of Integrative Physiology, Department of Physiology and Pharmacology, Karolinska Institutet, Stockholm, Sweden. *A full list of affiliations appears at the end of the paper. ✉e-mail: asbanks@bidmc.harvard.edu

The International Indirect Calorimetry Consensus Committee (IICCC)

Alexander S. Banks[1], David B. Allison[2], Thierry Alquier[3,4], Ansarullah[5], Steven N. Austad[6,7], Johan Auwerx[8], Julio E. Ayala[9,10], Joseph A. Baur[11,12], Stefania Carobbio[13], Gary A. Churchill[5], Morten Dall[14], Rafael de Cabo[15], Jose Donato Jr.[16], Nathalia R. V. Dragano[17,18], Carol F. Elias[19,20], Anthony W. Ferrante Jr.[21], Brian N. Finck[22], Jose E. Galgani[23,24], Zachary Gerhart-Hines[14], Laurie J. Goodyear[25], Justin L. Grobe[26,27,28,29], Rana K. Gupta[30], Kirk M. Habegger[31], Sean M. Hartig[32,33,34], Andrea L. Hevener[35,36], Steven B. Heymsfield[37], Corey D. Holman[38], Martin Hrabě de Angelis[17,18], David E. James[39,40,41], Lawrence Kazak[42,43], Jae Bum Kim[44], Martin Klingenspor[45], Xingxing Kong[46], Sander Kooijman[47,48], Louise Lantier[9,10], K. C. Kent Lloyd[49,50], James C. Lo[51,52,53], Irfan J. Lodhi[54], Paul S. MacLean[55], Owen P. McGuinness[10], Gema Medina-Gómez[56], Raghavendra G. Mirmira[57], Christopher D. Morrison[58], Gregory J. Morton[59], Timo D. Müller[60,61], Yoshihiro Ogawa[62], David Pajuelo-Reguera[63], Matthew J. Potthoff[64,65], Nathan Qi[19], Marc L. Reitman[66], Patrick C. N. Rensen[47,48], Jan Rozman[67], Jennifer M. Rutkowsky[68], Kei Sakamoto[14], Philipp E. Scherer[69], Gary J. Schwartz[70,71], Radislav Sedlacek[63], Mohammed Selloum[72], Saame Raza Shaikh[73], Shuai Chen[74,75], Gerald I. Shulman[76], Vojtěch Škop[77,78], Alexander A. Soukas[79,80], John R. Speakman[81,82,83,84], Bruce M. Spiegelman[85,86], Gregory R. Steinberg[87,88], Katrin J. Svensson[89,90,91], John P. Thyfault[92,93,94], Tony Tiganis[95,96], Paul M. Titchenell[11,12], Nigel Turner[97,98], Licio A. Velloso[99], Antonio Vidal-Puig[100,101,102,103], Christopher S. Ward[104], Ashley S. Williams[30], Christian Wolfrum[105], Allison W. Xu[106,107], Ying Xu[108] & Juleen R. Zierath[14,109,110]